Title: Laser Processing of Bulk Metallic Glass: A Review

Author: E. Williams N. Lavery

PII: S0924-0136(17)30127-9
DOI: http://dx.doi.org/doi:10.1016/j.jmatprotec.2017.03.034
Reference: PROTEC 15177

To appear in: *Journal of Materials Processing Technology*

Received date: 6-10-2016
Revised date: 14-3-2017
Accepted date: 30-3-2017

Please cite this article as: Williams, E., Lavery, N.,Laser Processing of Bulk Metallic Glass: A Review, *Journal of Materials Processing Technology* (2017), http://dx.doi.org/10.1016/j.jmatprotec.2017.03.034

Laser Processing of Bulk Metallic Glass: A Review

E. Williams [(a)*] and N. Lavery [(b)]

(a) Cardiff School of Engineering, Cardiff University, Cardiff CF24 3AA, UK

(b) College of Engineering, Swansea University, Bay Campus, Fabian Way, Swansea, SA1 8EN

* Corresponding author. E-mail address: eleri.williams89@gmail.com

Abstract

The emergence of bulk metallic glasses and their identification as versatile advanced engineering materials with attractive properties has led to a surge in research efforts to investigate processing methods, which can be used either to synthesise new BMG alloys or to shape BMG workpieces into final components with specific geometries. Among such technologies, the number of studies focussing on the laser processing of BMGs has gradually increased over the past decade. For this reason, a comprehensive summary of the state-of-the-art in this particular field of research is presented in this review. The reported studies are categorised into the different laser applications that have been proposed so far by the research community, namely the welding, cladding, additive layer manufacturing, micro machining and microstructure modification of BMG substrates. Due to the attractive properties of BMGs stemming from their amorphous nature, results are also presented, when available, concerning the effect of laser irradiation on the generation of crystalline precipitates during processing and the effect of these changes on the resulting material properties. This review has identified a number of gaps in the knowledge surrounding the laser processing of bulk metallic glasses. Understanding the fundamental interaction of laser energy with multi-component alloys will be necessary, as the development of lasers continues and the amount of available

bulk metallic glasses increases. In particular, the crystallisation kinetics of bulk metallic glasses during laser irradiation needs to be understood to aid in the development and optimisation of processes such as welding and cladding. This could be helped by created an accurate simulation model to predict the onset of crystallisation although this is not a minor challenge, developing a complete temperature field model during laser irradiation is a complex task when considering vaporisation, plasma effects as well as chemical composition changes in the material. Besides, there is also the issue of variations in material properties as the temperature increases, particularly for BMGs whose temperature dependent properties are not well-documented. The research into the additive layer manufacturing of bulk metallic glass should continue to grow. Parametric effects need to be addressed to complete the optimisation of this process. Further investigations of the resulting crystallisation processes upon repeated melting and solidification should also aid in the process being able to be controlled more effectively. Finally, the use of laser processing of bulk metallic glass for specific application needs to be investigated further.

Keywords

Bulk metallic glasses; amorphous alloys; laser welding; laser cladding; additive layer manufacturing; laser processing review.

1. Introduction

Bulk metallic glasses are an emerging family of advanced engineering materials that have inherent attractive properties, ranging from their superior hardness, good corrosion resistance to a large elastic strain limit **(Peker and Johnson, 1993)**. In the last decade, a number of reviews have been published related to the synthesis, properties and applications of this class of materials. The review by **Axinte (2012)** discussed the history of bulk metallic glasses, their properties and their applications. The author concluded that the future for these materials was destined to be bright with advances in thermoplastic forming and specially designed structural bulk metallic glasses predicted. **Schroers (2010)** presented a detailed review of the processing of bulk metallic glasses, including the casting and thermoplastic forming and their effect on the material properties. **Lu and Liu (2004)** reviewed the role of minor alloying additions during the formation of bulk metallic glasses, presenting the effect on various types of alloying on the material properties. In order to complement the information reported in these reviews, the specific aim of this paper is to present the current state-of-the-art in the processing of bulk metallic glasses using laser given that this is a field of research which has gained increased interest in the last decade.

In 1960 the first metallic glass was reported by a group at California Institute of Technology (**Klement et al 1960**) and their development was continued by Chen et al during the 1970s. This new material had the internal amorphous structure of a glass whilst its constituent parts were metallic elements. In order to develop these materials, the liquid phase of the metallic elements is cooled as quickly as possible, quicker than a specific critical cooling rate. Cooling quicker than this rate results in free atoms not having enough time to organise

themselves into an ordered metallic lattice. Needing a very high cooling rate to create these disordered lattice restricted early fabrication attempts to very thin dimensions to allow fast heat dissipation.

Today, a number of different amorphous metallic alloys can be produced with dimensions in the range of a few centimetres such as those reported by **Inoue and Takeuchi (2011)** in Figure 1.1.

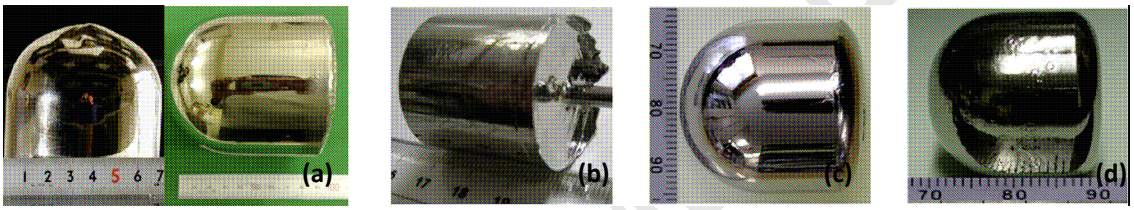

Figure 1.1. Different types of bulk metallic glass ingots (a) Pd-Cu-Ni-P, (b) Zr-Al-Ni-Cu, (c) Cu-Zr-Al-Ag and (d) Ni-Pd-P-B (Inoue and Takeuchi, 2011).

Table 1.1 displays a comparison between the properties of metals, glasses and metallic glasses.

These properties make bulk metallic glasses ideal candidate for many different applications across many industrial sectors, as reported by Inoue et al 2011.

Property	Metal	Glass	Metallic Glass
Structure	Crystalline	Amorphous	Amorphous
Interatomic Bonding	Metallic	Covalent	Metallic
Yield Stress	Non-ideal	Almost-ideal	Almost-ideal
Hardness	Various	Very high	Very high
Optical Nature	Opaque	Transparent	Opaque
Conductivity	Good	Poor	Very good
Resistance	Low	High	Very low
Corrosion Resistance	Various	Very good	Very good
Magnetic Properties	Various	None	Various

Table 1.1 Comparison of the properties of metals, glasses and metallic glasses.

(Adapted from Anantharaman 1984).

The amorphous structure of a material with the properties of metal results in the unique ability to form bulk metallic glasses like plastic. **Schroers et al (2007)** were able to process BMG with thermoplastic forming for MEMS fabrication by raising the temperature of the material in the super cooled liquid region for a duration short enough to avoid the onset of crystallisation. They concluded that being able to replicate 100 nm features in a similar way to plastic but with a material that has a high-strength, produces a wide range of applications for microstructures and MEMS fabrication. This ability to be formed like plastic also provides

interesting prospect to the biomedical industry, as BMGs exhibit a strength and elasticity that exceeds most biomaterials. In particular, **Schroers et al (2009)** conducted biocompatibility tests and concluded that a number of BMGs could be used successfully as biomedical implants.

The versatility of laser processing and the desirable properties of bulk metallic glasses have resulted in a variety of publications focusing on laser welding, cladding and coating and the more recent development of additive layer manufacturing of bulk metallic glass structures. The use of lasers to process bulk metallic glass will ultimately produce heating and cooling cycles within the material. Due to the properties of BMGs being directly linked with their amorphous structure, it is desirable for these heating and cooling cycles to be within a range whereby they do not induce crystallisation precipitates into the microstructure of the material. Glass forming ability (GFA) characterises the ability of a BMG to withstand crystallisation. **Greer (2015)** states that this property will scale inversely with the cooling rate induced in a BMG. This means that a higher cooling rate necessary to avoid crystallisation within a particular BMG, the lower its GFA. With respect to laser processing, if the material has a low GFA then the cooling rate necessary to keep its amorphous structure will be high, possibly too high for the cycles induced during processing. Figure 1.2 from the work of **Pauly et al (2013)** describes the continuous-cooling (CC) diagram for the specific BMG studied. If the cooling curves induced during laser processing intercept with the CC curves for the BMG then crystallisation may occur.

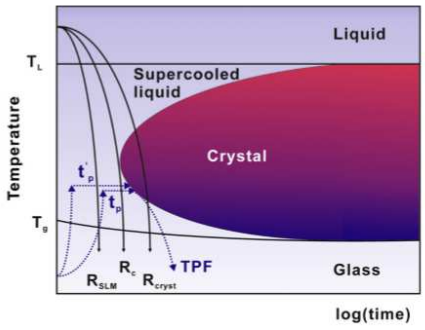

Figure 2.1. A schematic diagram of the continuous cooling curve for bulk metallic glasses (Pauly et al, 2013).

In this context this review aims to present recent research on the laser processing of bulk metallic glass, in particular laser welding, cladding, additive layer manufacturing, micro machining, and the use of laser processing to deliberately alter the properties of the BMG material. The review will focus on laser processing of bulk metallic glasses although laser processing of thin metallic glass samples has also been conducted. In particular, Zheng et al (2013) studied the dynamic fracture behaviour of Fe-based metallic glass having used lasers to produce a shock load and Otsu et al (2009) utilised YAG lasers to bend a thin sample of palladium based metallic glass without crystallisation. Finally, concluding remarks concerning the future of laser processing of bulk metallic glasses are provided in the last section.

2. LASER WELDING OF BULK METALLIC GLASSES

2.1 Introduction to laser welding

Laser welding utilises high energy laser beams, scanned across the surface of two adjacent materials, to create a small diameter keyhole where the material has been vaporised. Within this keyhole, the vapour pressure prevents the molten wall, created when the laser beam scans the material, from collapsing. As this keyhole is moved along the surface it

leaves a trail of molten material which forms the seal between the two joined materials. Figure 2.1 shows a schematic of how laser keyhole welding operates in practice (**Dawes, 1992).**

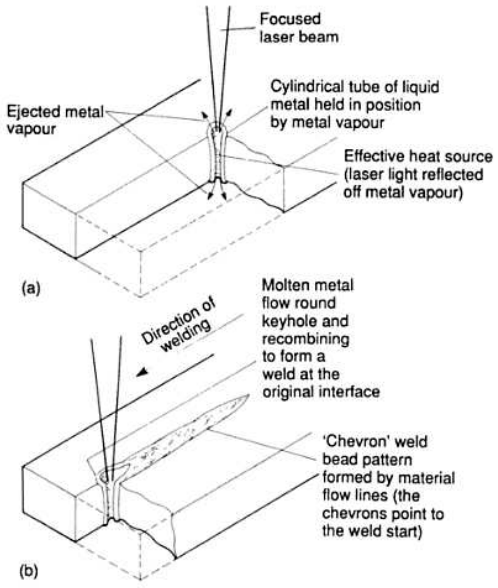

Figure 2.1. The process of laser welding; the absorption of the focused laser beam causes material to be evaporated creating a keyhole which is held open by the vapour pressure within the cavity. The beam is then moved across the weld joint leaving a trail of solidified molten material (Dawes 1992).

For bulk metallic glasses, laser welding is particularly useful. This is due to the fact that the size restrictions associated with the production of BMG components means the development of a successful joining technique is a necessary pre-requisite to widen the range of engineering applications for BMGs **(Kim et al 2006)**. When utilising laser welding for bulk metallic glasses, the quality of the weld is not only measured in weld-beam geometry, mechanical properties and distortion **(Khan et al 2011)** but also on the resulting micro structure and whether it remains amorphous after processing. The fast heating and

cooling rates associated with laser processing can aid in the avoidance of crystallisation within the weld seam which allows a processed BMG to retain its desirable properties. Therefore, the successful laser welding of bulk metallic glasses relies on analysis on the relationship between laser parameters and the resulting weld seam quality as well as that between laser parameters and the resulting material micro structure and in particular if changes to this micro structure affect the resulting strength of the weld.

2.2 Effect of varying laser processing parameters on crystallisation of bulk metallic glass.

Due to the flexibility of laser processing there are a large number of parameters that can affect the machining outcomes of welding bulk metallic glass. **Li et al (2006)** investigated the effect of varying the scanning speed from 2 to 8 $m.min^{-1}$, using a peak output power of 1200 W, on the crystallisation of the weld bead and the heat affected zone when joining two pieces of a $Zr_{45}Cu_{48}Al_7$ bulk metallic glassy alloy measuring 1 mm in thickness, 5 mm in width and 15 mm in length. After processing, the structure of the substrate was investigated using X-ray diffractometry (XRD) and an optical microscope and the difference in thermal properties was analysed using differential scanning calorimetry (DSC). Through these techniques it was observed that crystallisation was only occurring during the processing with slower scan speeds. This effect can be seen in the XRD results from the authors shown in Figure 2.2 along with the areas of the weld studied. The authors concluded that the higher welding speed resulted in a cooling rate that was high enough to suppress crystallisation. Also, these authors suggested that the crystallisation in the weld pool and the heat affected zone (HAZ) occur due to different reasons. Within the HAZ, crystallisation was dependent on the amount of time the temperature was raised above the crystallisation temperature of the material whereas, the crystallisation in the weld pool was based on the

cooling rate from the melt temperature to the glass transition temperature.

(i).

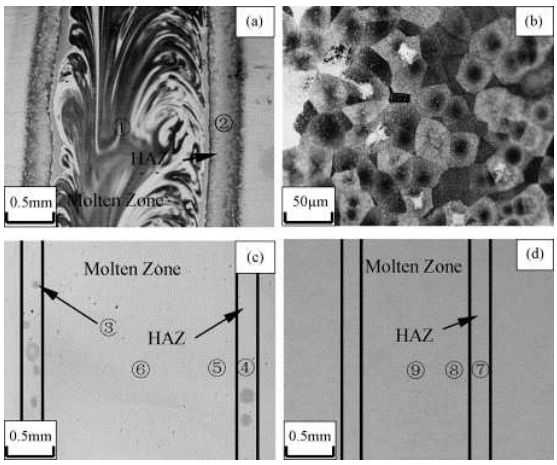

(ii).

Figure 2.2. (ii) XRD results for the welding of $Zr_{45}Cu_{48}Al_7$ at the numbered areas shown in (i) at differing scan speeds of (a,b) 2m/min, (c) 4 /min and (d) 8 m/min (Li et al 2006).

This conclusion was supported by the development of a finite element heat source model. In particular, the temperature profiles created from this model showed that the samples, which were scanned more slowly, remained above the crystallisation temperature long enough for the sample to crystallise. This study highlights the effect that varying the laser processing parameters has on the resulting thermal cycles within the material and how these difference affect the ability of the material to remain amorphous after welding. However, the authors only varied the scanning speed during their investigations without addressing other potential parametric effects such as changes in pulse duration or energy.

A study by **Kim et al (2006)** provided further understanding regarding the evolution of the BMG structure during welding when subject to parametric variation of the laser system used

to process it. These authors used an Nd:YAG laser system to weld a copper based bulk metallic glass ($Cu_{54}Ni_6Zr_{22}Ti_{18}$). Unlike **Li et al (2006),** this work incorporated variations in the peak power, pulse duration, frequency and travel speed. Analysis of the microstructure after welding was conducted using XRD, scanning electron microscopy (SEM), transmission electron microscopy (TEM) and DSC. In addition a thermocouple was used to record the temperature during irradiation during processing as well as a theoretical approach to estimate the thermal profiles. Using these methods, it was concluded that the higher the pulse energy and the longer the pulse durations were, the more likely the bulk metallic glass was to crystallise due to 1) the lower cooling rates achieved and 2) the variation in chemical composition of the material with the vaporisation of copper at the higher temperatures reached when the pulse energy increases.

Another conclusion reported, by these authors, was that the analysis of the crystallisation using single pulses could not be used to predict the crystallisation behaviour upon irradiation with multiple pulses due to the pre and post-heating effects of the interacting laser pulses. This is illustrated in Figure 2.3 which presents the estimated temperatures at two points in the HAZ for two different pulse repetition frequencies. More specifically, this figure shows that a second pulse can irradiate when the temperature has already been increased by a preceding pulse. This condition is mostly affected by the frequency of the single pulses, which directly affects the pulse-to-pulse interaction. This conclusion is important with respect to the theoretical prediction of crystallisation behaviour because it means that a theoretical model for only a single pulse will be insufficient and provisions will have to be made for overlapping, moving pulses. Also, it displays potential difficulties faced when welding using a pulsed laser source rather than a continuous wave source, which essentially eradicates the issue of pulse to pulse interactions and varying thermal cycles.

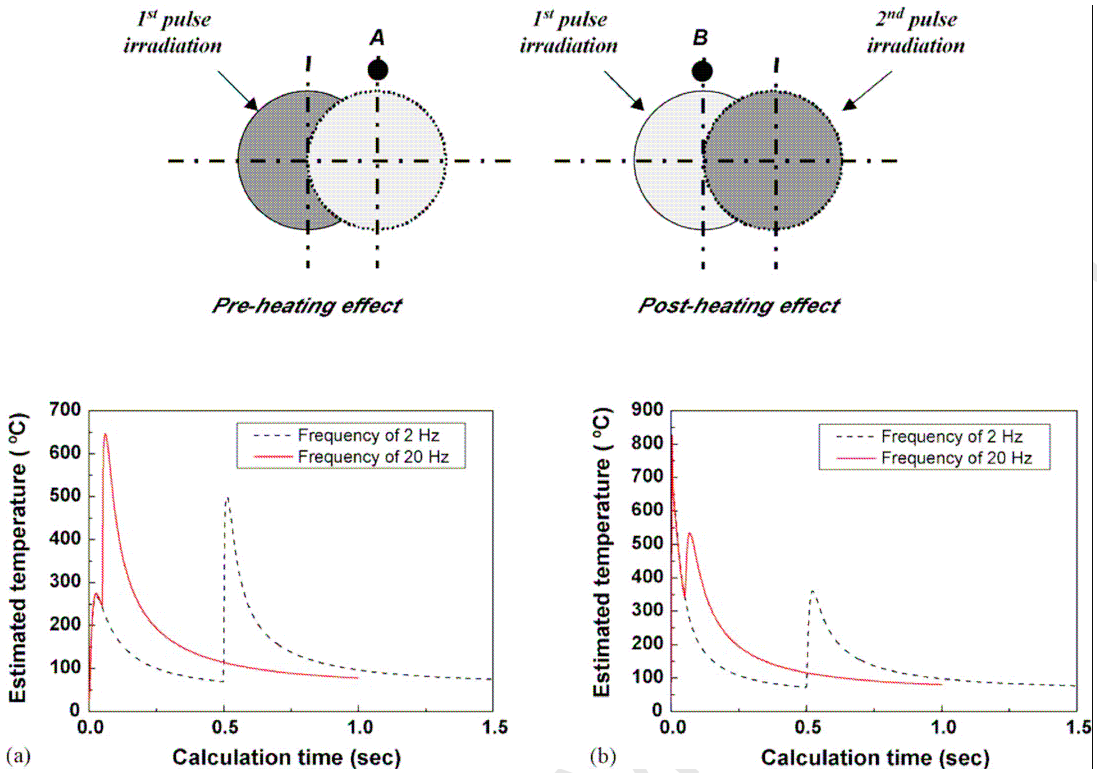

Figure 2.3 Effect of pre-heating and post-heating on the temperature in the heat affected zone during pulsed laser welding (Kim et al 2006).

Kawahito et al (2008) shifted the attention to focus on fast i.e 48 and 72 m.min^{-1}, high-power fibre laser welding of a 1 mm thick Zr-based bulk metallic glass ($Zr_{55}Al_{10}Ni_5Cu_{30}$). Similarly to previous studies, the experimental focus was on the ability to retain the amorphous structure in the weld joint so as not to affect the desirable mechanical properties of the alloy. It was concluded, through XRD analysis of the weld bead, that the higher scanning speed of 72 m.min^{-1} allowed a full weld to be obtained as well as retaining the amorphous structure of the BMG. Although the weld was also of acceptable quality for the slower scan, the XRD pattern displayed peaks of crystalline precipitates within the weld

seam. Even though this work did not investigate all the parametric variations the high-power fibre laser system is capable of during the welding of BMGs, it is a demonstration of the applicability of this specific generation of lasers to BMG processing.

After the initial interest in laser welding of BMGs the amount of research increased to include many different types of BMGs with varying compositions. Further investigations of the Nd:YAG welding of Zr-based bulk metallic glass ($Zr_{53}Cu_{30}Ni_9Al_8Si_{0.5}$) was conducted by **Wang et al (2010).** Using three different parametric conditions, defined by different peak power, pulse duration and laser energy, the structure of each different area composing of the weld pool, i.e the HAZ and the parent material, was analysed using SEM, XRD, TEM and electron diffraction spectroscopy (EDS). In agreement with both **Li et al (2006)** and **Kim et al (2006)**, it was stated that the crystallisation in the weld pool and the HAZ occurred due to different reasons. In particular, crystallisation in the HAZ depended on how long the temperature was above the crystallisation temperature whereas the weld pool displayed crystallisation based on the rate of cooling between the melt temperature and the glass transition temperature where atoms lose their translational motion. A magnified imaged of the precipitates formed in the HAZ for each sample is shown in Figure 2.4 along with a table of the atomic percentage of each element present in the precipitates.

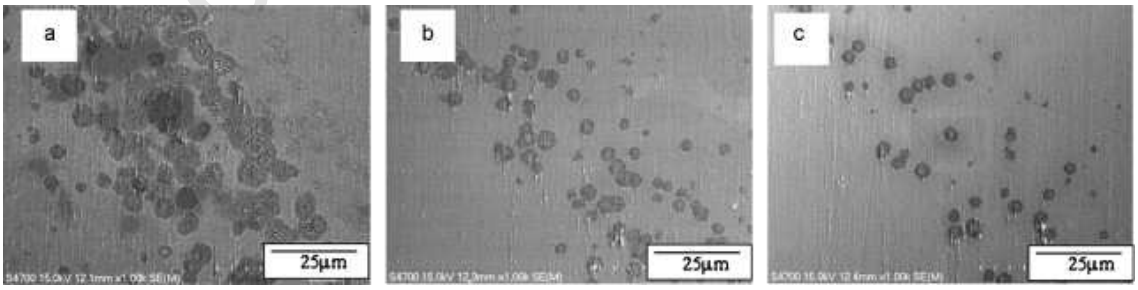

Sample	Region	Zr	Ni	Cu	Al

Sample	Region	Zr	Ni	Cu	Al
A	Precipitates in the HAZ	28.60	15.79	50.89	4.72
B	Precipitates in the HAZ	36.62	13.15	45.33	4.91
C	Precipitates in the HAZ	39.91	14.45	41.60	4.04
A	WFZ	52.59	11.80	26.95	8.66
B	WFZ	51.08	13.06	26.93	8.93
C	WFZ	54.19	11.04	27.72	7.05
PM	Unaffected zone	51.91	9.5	31.32	7.26

Figure 2.4. A magnified image of the spherical crystalline precipitates formed in the HAZ in samples of work from Wang et al 2010 along with a table of the atomic percentage of each element within the crystalline structures.

The implications of pulse-to-pulse interaction were also discussed similarly to **Kim et al (2006).** Through experimental analysis, it was concluded that, with the parameters used in this investigation, crystallisation in the HAZ was inevitable. It was observed that the precipitates present after welding in the HAZ were rich in Zr, Ni and Cu with particle sizes varying from 30 to 200 nm.

Wang et al (2012) also studied the crystallisation of BMGs during the laser welding process. In this case the bulk metallic glass investigated was a $Ti_{40}Zr_{25}Ni_3Cu_{12}Be_{20}$ substrate. The laser used had a power of 3.5 kW and the scanning velocity ranged from 6 to 10 $m.min^{-1}$. These authors observed that the crystallisation in the weld joint, where the material is melted, and crystallisation in the HAZ, where the material stays solid, are dependent on different parts of the heating-cooling cycle. The authors concluded that the cooling rate from the melt temperature to the glass transition temperature is the decisive rate for the determination of the resulting microstructure of the weld zone which is in-line with earlier studies reported

above. In the case of the work of **Wang et al (2012),** the cooling rate needed to be larger than 780 K/s to avoid crystallisation of the substrate. On the other hand, the change in amorphous structure in the HAZ, which do not change phase, was said to depend on the entire heating and cooling cycle. In particular, if the HAZ is subject to a temperature above the glass transition temperature of the material for a relatively large amount of time then it is likely to display crystallisation. In agreement with **Li et al (2006)**, the faster scanning speeds resulted in retaining the amorphous structure, whilst the slower scanning speeds led to the material being subjected to a large temperature gradient for longer, causing crystallisation to become apparent. The authors also concluded that when amorphous, the welded joint exhibited almost the same tensile strength as that of the base material.

Being able to join bulk metallic glass substrates together is not the only important conclusion of laser welding research, it is also important to identify the differences in processing responses between bulk metallic glass alloys with varying elemental compositions. For example, **Wang et al (2013)** studied the effect of nickel content in a bulk metallic glass composite. A lack of nickel was suggested to improve the glass forming ability of this particular alloy composition. This was supported in the experimental results present by these authors. At the same time, the BMG that contained nickel displayed evidence of crystallisation during laser welding, whilst the nickel-free composition did not. This lack of crystallisation in the nickel-free material meant that the micro-hardness of the welded substrate remained high as did the glass forming ability.

Most recently the studies of laser welding of BMG's have evolved to include welding of BMG-composites, BMGs created with reinforced crystalline phases embedded in the glassy matrix to improve the ductility of these otherwise strong materials. **Wang et al (2016)**

concluded that welding a Zr-based BMG with a high % volume of Ta resulted in similar characteristics to those observed when welding the same material without the addition of Ta.

2.3 Avoiding crystallisation during laser processing

Having identified that crystallisation can occur during laser welding **Wang et al (2010_b)** attempted to combine the welding with a liquid cooling device to decrease the initial weld temperature in order to increase the cooling rate so as to avoid crystallisation during welding. Further research by the authors **(Wang et al 2011)** uses the same liquid cooling device to control the start temperatures of the material to determine the effect on the crystallisation behaviour of the welding of a Zr-based BMG with a 4.5ms Nd:YAG laser. It was found that decreasing the initial weld temperature did increase the cooling rate and resulted in a smaller amount of crystalline precipitates formed within the heat affected zone. The calculated cooling rates for each different temperature are shown in Table 2.1.

Conditions	A	B	C	D	E	F
R_{T_m/T_g} (ms)	2.3×10^2	1.7×10^2	89	83	81	79

Table 2.1. Calculated cooling ranges for each parametric combinations with different initial welding temperature during the welding of Zr-based bulk metallic glass (Wang et al 2011)

On the subject of temperature variation prior to welding, **Chen et al (2014)** applied thermal annealing prior to the welding of $Zr_{55}Cu_{30}Ni_5Al_{10}$. It was concluded that the annealing at a temperature a little above the glass transition temperature of the material was beneficial to the weld quality, improving the micro-hardness and bending strength of the welded area.

2.4 Theoretical simulation of laser processing of bulk metallic glass

It is useful to use experimental trial and error to determine laser processing parameters that lead to crystallisation when employing laser welding to join bulk metallic glass substrates but this method can be incomplete in its analysis, as well as costly. In order to avoid this, prediction of crystallisation during laser welding using theoretical analysis can be utilised. **Li et al (2006)** developed a theoretical model which was described in section 2.2. In the work by **Kim et al (2006)** it was suggested that to achieve welding that avoids crystallisation of the material there is a crystallisation start line in the temperature profiles of the material undergoing processing that provides the heating and cooling rates necessary to avoid crystallisation. **Xia et al (2009)** provided an extension to this work by creating an effective method that can identify this start line by predicting the thermal cycles of a Zr-based BMG at various points within the weld area. The theoretical temperature predictions at the boundary between the weld heat affected zone and the unaffected material were used to determine the tangential points where the crystallisation start line would be created. This can be seen in Figure 2.5.

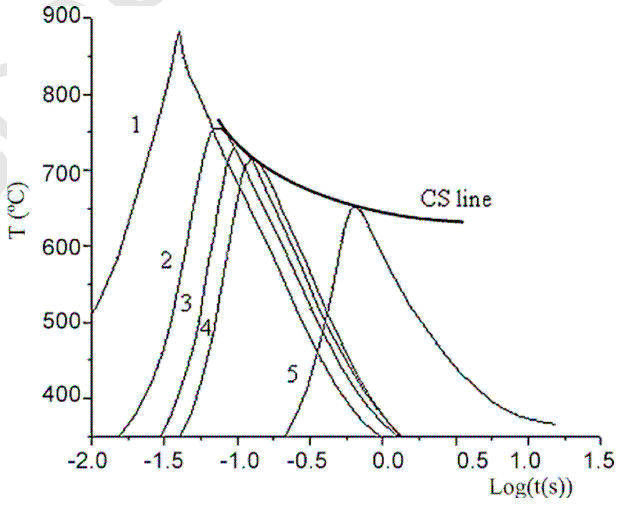

Figure 2.5. The theoretical predictions of the temperature evolution with time and the boundary by which the crystallisation start time can be predicted (Xia et al 2009).

Chen et al (2015) have incorporated Kissinger analysis as well as temperature field simulation. By comparing the continuous heating transformation curve with the temperature profiles simulated, it is possible to predict when these interact, thus leading to crystallisation during the welding process. It was concluded that this intersect would occur in samples welded with a low scan speed or a high power. An example for one sample is shown in Figure 2.6. This conclusion was verified using experimental analysis of Zr-based bulk metallic glass processed under the same conditions.

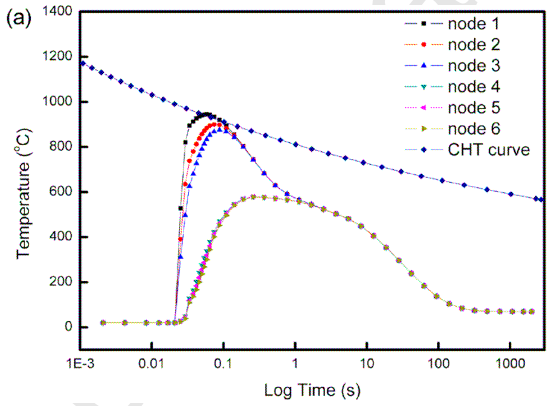

Figure 2.6. Simulated temperature profiles and predicted critical cooling curve (Chen et al, 2015).

3. LASER CLADDING/COATING OF BULK METALLIC GLASSES

3.1 Introduction to laser cladding and coating

Laser cladding works by using a focused beam of photons to melt a pre-deposited powder onto the surface of a substrate material. The rapid heating and cooling induced during laser processing results in minimal thermal effects on the base material during laser cladding **(Toyserkani et al 2004).** To create an optimal clad layer using a laser there are many factors to consider such as the effect of material properties on the absorption and melt pool

geometry as well as the laser parameters which can affect the clad dimensions and microstructure. As well as these factors, when laser cladding with metallic glasses there is the added dimension of retaining the amorphous structure of the coating throughout its thickness. Even so laser cladding created the possibility of exploiting the desirable properties of bulk metallic glasses to improve the surface characteristics of many manufactured components that are only functional at their surface **(Matthews et al 2007).**

3.2. Early cladding and coating of bulk metallic glasses

In 1997 **Wong and Liang** presented an exploratory study reporting on the coating of Al-Si surfaces with amorphous Ni-Cr-B-Si material. This work was extended by **Wong et al** in 2000. It was concluded that laser cladding resulted in a higher hardness and wear resistance than the Al surface.

Having shown that creating a partially amorphous layer was possible using laser cladding, **Wu and Hong (2001)** moved on to increasing the thickness of the coating to 1.2mm. The authors used a Fe-based bulk metallic glass and clad using a 10 kW continuous wave CO_2 laser in a shielding box with a supply of argon gas to obtain a positive gas pressure. It was concluded that the high cooling rate produced during laser cladding was sufficient to induce a layer of amorphous alloy coating of 1.2 mm in thickness with a high glass-forming ability. A micrograph of the coating can be seen in Figure 3.1. This property was characterised by the large super-cooled liquid region determined by the DSC measurements of the crystallisation temperature and the glass transition temperature.

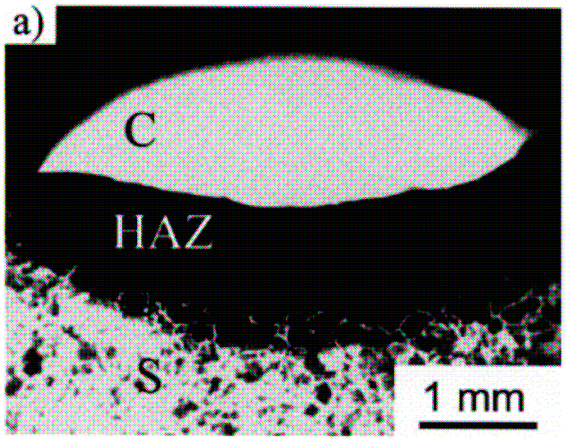

Figure 3.1. An optical micrograph of an Fe-based BMG 1.2mm thick coating and its corresponding heat affected zone (Wu and Hong 2001).

3.3 Properties of laser clad layers of bulk metallic glass

After the initial support in favour of the creation of amorphous coatings with a high glass-forming ability, research was focused toward the actual properties of such layers. **Wang et al (2004)** attempted to increase the tribological performance of crystalline titanium by laser cladding with a Zr-based bulk metallic glass. The BMG powder was pre-deposited on the surface of the titanium substrate before being clad by a CO_2 laser operating with a 5 mm beam diameter at 1.4 kW and scanning at $4mm.s^{-1}$. After a single laser scan, the laser clad layer was analysed using multiple techniques including XRD, SEM and TEM. The analysis first concluded that the 1 mm layer of BMG was not entirely amorphous with crystalline precipitates throughout the layer, consisting mainly of Zr- bonded phases such as Zr_3Al_2. It was also observed that the microstructure of the layer varied depending on the distance from the parent material. This was due to the variation in heating gradients observed throughout the layer depth. These differences in heating gradients affected the apparent crystallisation throughout the depth and the resulting micro-hardness as can be seen in Figure 3.2. Not only did the different thermal gradients affect the crystallisation but the

chemical composition change at the titanium surface resulting from the mixing of the molten parent material and the molten BMG powder created ideal conditions for nucleation and growth of crystals. Even though the layer was not completely amorphous, the micro-hardness increased compared to a fully amorphous substrate and the friction coefficient was also lower than a fully amorphous comparison.

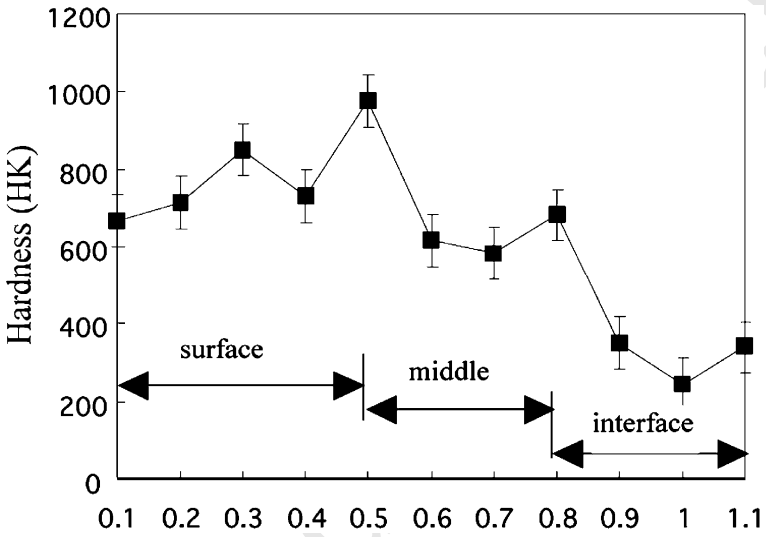

Figure 3.2. Variation in hardness throughout the laser clad coating as a result of the difference in microstructure occurring due to a variation in the thermal gradients (Wang et al 2004).

3.4 Improving the cladding process

In order to attempt to avoid any crystalline precipitates being formed in the clad layer, it is possible to avoid melting the amorphous powder by using a blown-powder method, whereby the laser is used to create a melt pool on the surface of the substrate material and then the powder is deposited into this pool. **Yue et al (2007)** used this method to clad a layer of 1.5 mm in thickness composed of $Zr_{65}Al_{7.5}Ni_{10}Cu_{17.5}$ onto the surface of commercially-pure magnesium. This research was an attempt at improving the wear and corrosion characteristics of magnesium parts which hinder their wide-spread application.

Having analysed the laser-clad layer, it was concluded that it was fully amorphous up to a depth of 1.1 mm and it had bonded well with the magnesium substrate. Also, unlike the two step method as utilised by **Wang et al (2004)**, this method resulted in less variation of the hardness throughout the clad layer. Finally, the layer improved both the wear and corrosion characteristics of the surface, compared to both the un-coated magnesium surface as well as surfaces coated with other materials.

It is not only the method of laser cladding that affects the overall functionality of the surface; **Li et al (2011)** investigated the effect of variations in the ratio of nickel to iron, in the BMG composite Ni-Fe-Si-B-Nb, on the properties of the laser clad coating of mild steel. The coatings were clad with varying percentages of Ni from 45% to 60% using the two step powder deposition and remelting method. The layer was then remelted using a higher scanning speed. It was observed that the microhardness varied with the depth of the layer (c.f. Figure 3.3). It was observed that all powder compositions led to a predominately amorphous layer with embedded nano-crystals the compositions of which depended on the Ni-Fe ratio. Even though all of the coatings resulted in better properties than the uncoated substrate, the coating with a 1:1 ratio of Ni to Fe was superior to the other compositions. This was postulated to be due to the difference in microstructure, chiefly the increase in the amorphous fraction of the layer.

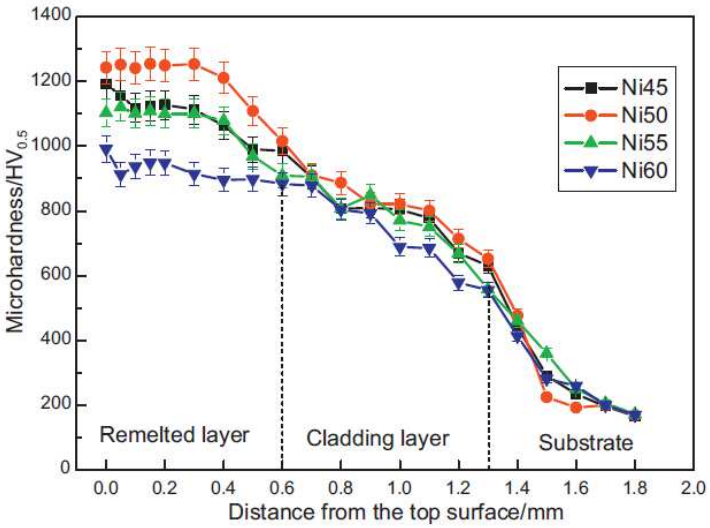

Figure 3.3. The variation in the micro-hardness throughout the depth of the remelted layer in four different BMG coatings with various percentages of Ni (Li et al, 2011).

In the reported literature above, laser cladding operations were conducted with the use of a shielding box filled with gas to prevent oxidation. This can limit the size and geometry of the material being clad. **Zhu et al (2013)** reported on the laser cladding of low carbon steel with an Fe-based bulk metallic glass using a one step process and eliminating the need for a shielding box. These authors utilised a high power diode laser with values of power, scanning speed and powder feed rate pre-selected via initial optimisation tests for high bonding strength and low dilution rate between the substrate material and the coating. Thus, values of 1200 W, 17mm.s^{-1} and 15.1g.min^{-1} were chosen for the laser power, scanning speed and powder feed rate respectively. The coating produced at these parameters was determined to have an amorphous content of 87.6% and, similar to the other conclusions reported earlier in this section, the clad layer displayed different morphologies as a function of the distance from the substrate shown in Figure 3.4.

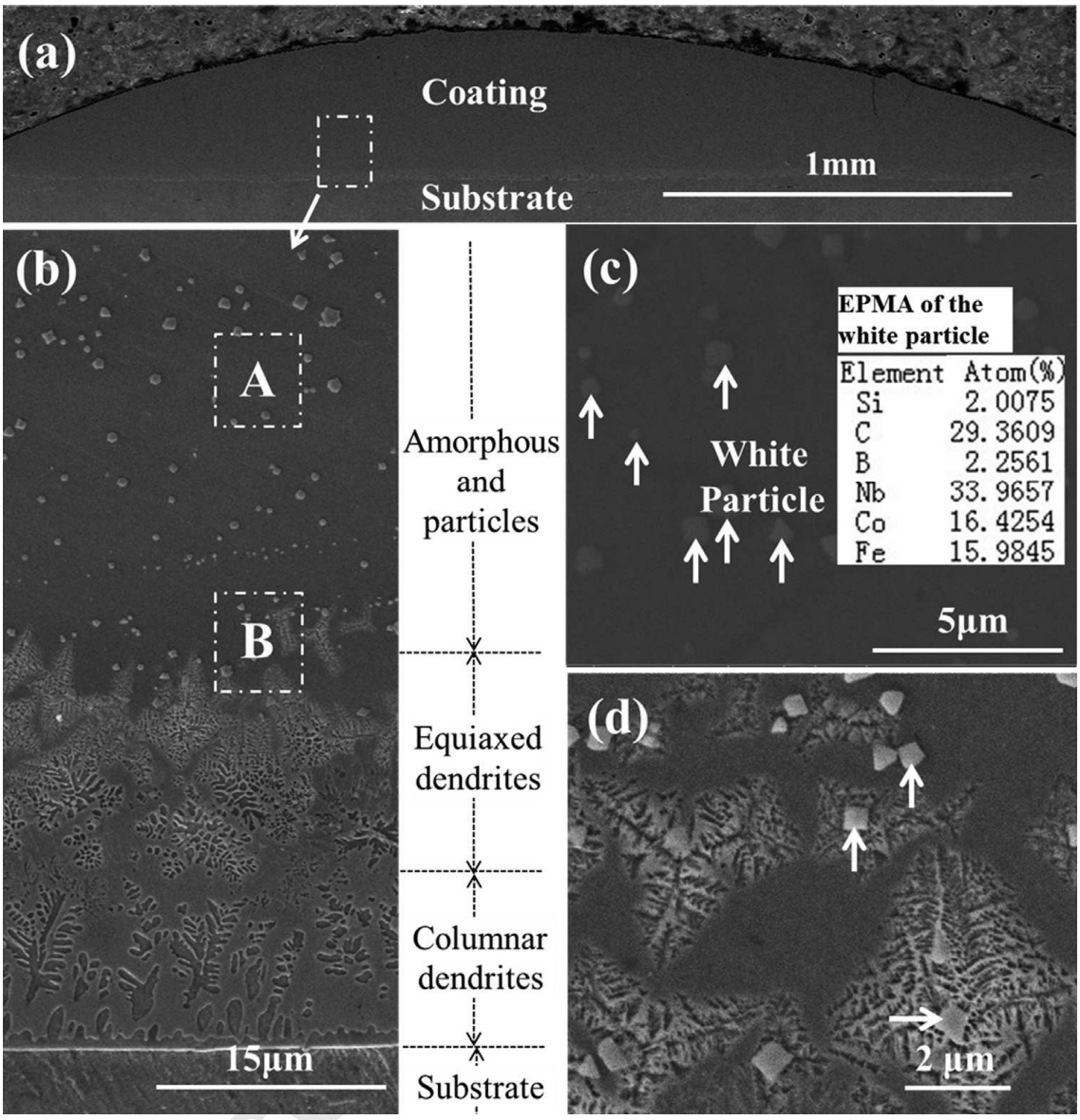

Figure 3.4. Variation in the micro-structure of the coating (Zhu et al 2013).

The authors concluded that the majority of crystalline particles were of the form NbC and that these particles contributed to the increase in hardness experienced after laser cladding. **Li et al (2013)** also commented on the observation of such particles when cladding mild steel sheets with a Ni-based bulk metallic glass powder, the XRD of this material after processing can be seen in Figure 3.5. It was noted that the reaction between the Nb and the elemental carbon creates a very stable compound that, due to its high melting point, is unlikely to melt during the laser cladding process resulting in an abundance of this

crystalline precipitate in the solidified layer. The authors of this research also indicated that the properties of the partially amorphous coating created during laser cladding are not superior to those inherent to its fully amorphous counterpart. This can cause problems during the lifetime of the clad layer.

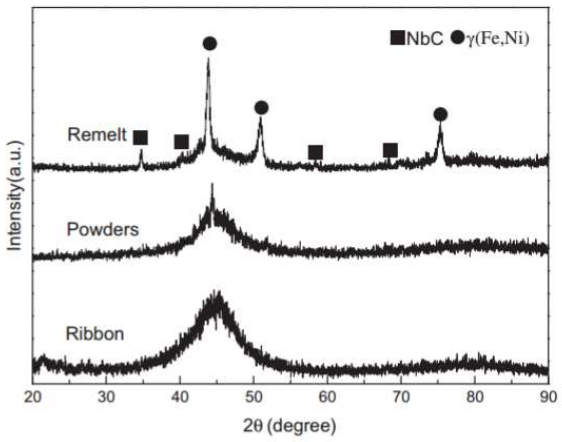

Figure 3.5. XRD of an Ni-based BMG composite coatings processed by laser (Li et al, 2013).

3.5. Simulation of the laser cladding/coating process

It is apparent from the existing literature that there are many different parameters that can affect the laser clad layer. **Yue et al (2007)** concluded that the method of cladding affects the homogeneity of the amorphous phase throughout the layer depth and **Zhu et al (2013)** observed the effect of varying the scanning speed, laser power and powder feed rate on the resulting mixing of the substrate material and the powder layer and the thickness of the layer itself. These relationships can be determined experimentally but this can be costly both in time and money. Simulating the process can be useful in predicting these relationships, thus reducing the costs involved. **Li et al (2014)** investigated the effect of scanning speed during the second laser melting process when cladding an Ni-based bulk metallic glass powder onto mild steel sheets using a high power diode laser. After the initial cladding was conducted, a second laser scan was run at values varying between 4m.min^{-1}

and 8 m.min^{-1}. As the laser was scanned over the surface of the coating faster, the thickness of the re-melted zone decreased. The faster the scan, the less heat is input into the surface. This affected not only the depth of the melt but also the microstructure. At faster scanning speeds, the heat input is small enough so as to not result in crystallisation of the coating. Using finite element modelling, the authors identified that the cooling rates at the slower scanning speeds were slow enough for the crystallisation process to take place. Figure.6 shows the results of the authors' simulation trials.

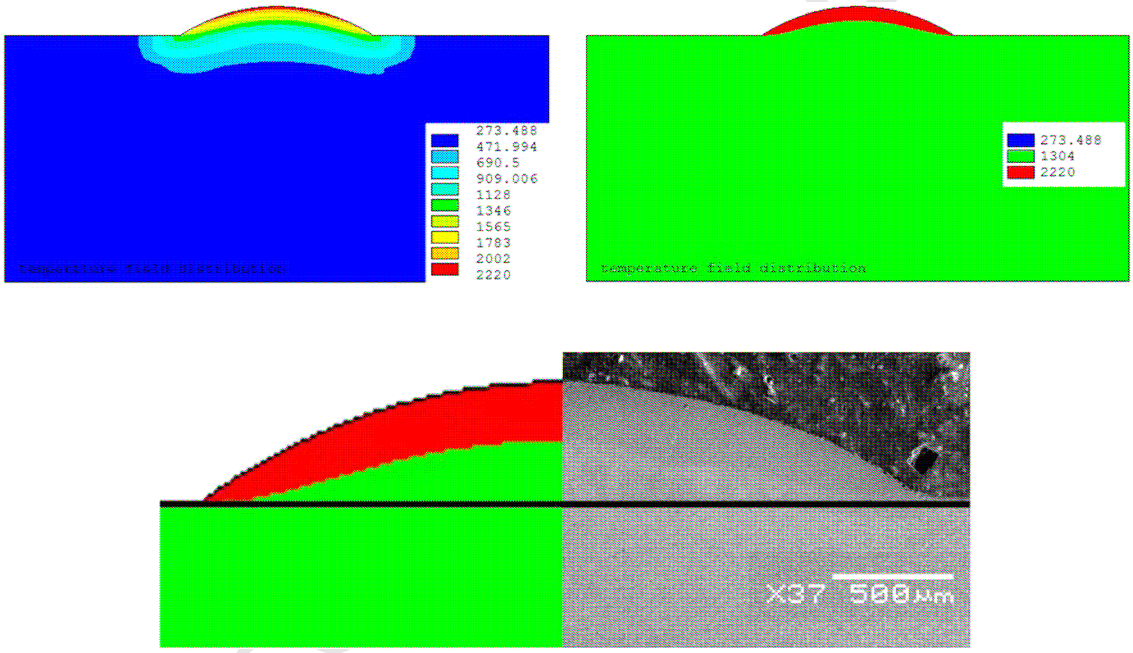

Figure 3.6 Simulation of the temperature field distribution during the laser cladding and remelting process and comparison with experimental images (Li et al 2014).

4. ADDITIVE LAYER MANUFACTURING OF BULK METALLIC GLASSES

4.1 Introduction to additive layer manufacturing

By integrating computer-aided-design and computer-aided manufacturing tools, the laser can be used to deposit layers of powder one on top of the other to produce functional net-shaped parts. This process is visualised in Figure 4.1. The global interest in additive layer

manufacturing (or 3D printing) has experienced a sharp incline in the past 5 years, mainly due to the expiration of key patents surrounding the technology. With the advancement of additive layer manufacturing technology and the desirable properties of bulk metallic glasses it would be an advantage to investigate this form of processing using such materials. Although bulk metallic glasses can be formed using thermoplastic forming to keep their amorphous structure, the processing time in the super cooled liquid region (SCLR) is limited to the duration which does not reach the crystal nucleation region. So to form complicated geometric shapes on a large scale the process has to either remove heat very quickly or it is limited by the SCLR requirements. This creates a necessity to explore other avenues of processing BMGs into complicated net shapes. The use of lasers to melt BMG powder layer by layer reduces the heating and cooling processes, which are constrained by the crystallisation kinetics of these materials, into cycles for each layer, allowing more freedom when creating net-shaped BMG components.

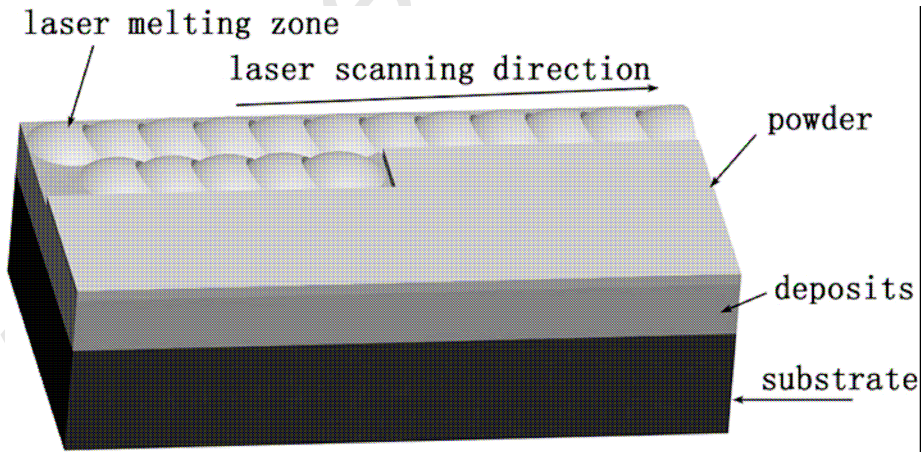

Figure 4.1. A visualisation of the additive layer manufacturing technique using a laser to melt a layer of powder that has been deposited on the surface of a substrate material. This

process is repeated over and over using the previous layer of solidified laser-melted powder as the surface for powder deposition (Yang et al 2012).

4.2. Initial additive layer manufacturing of bulk metallic glass

Yang et al (2012) investigated the possibility of forming 3-dimensional shapes out of Zr-based bulk metallic glass through repeatedly melting layer of its powdered form onto the previous layer. The tests were performed using an Nd:YAG laser operating at 3ms with a power of 300 W. The authors analysed structures made up of one, two, four and seven layers of melted powder. The results indicated that there was no crystallisation present until four layers were deposited, and even then the crystallised content was minimal with the amorphous contents being relatively high, at 92.44%. Through SEM analysis, it was determined that crystallisation did not occur throughout the layer but in specific areas identified as the heat affected zone of each layer. This zone was characterised through simulation as the area where the temperature rose above the glass transition temperature but not high enough to melt the material. It was concluded, via experimental and theoretical techniques, that, in order to maintain the amorphous structure in the layers, the accumulation of heat from one pulse to another and one layer to another must be low enough.

Pauly et al (2013) explored this process in more detail by using a Ytterbium fibre laser operating at 1064 nm and a maximum power of 400 W to create complex 3D structures (Figure 4.2) out of an Fe-based bulk metallic glass powder. Pre-experimentation was conducted to optimise the laser power (320 W), scanning speed (3470 $mm.s^{-1}$), track displacement (124 μm) and layer thickness (50 μm). It was observed that, although the final

structure was not entirely amorphous, it was no different than the original powder feedstock used in its creation

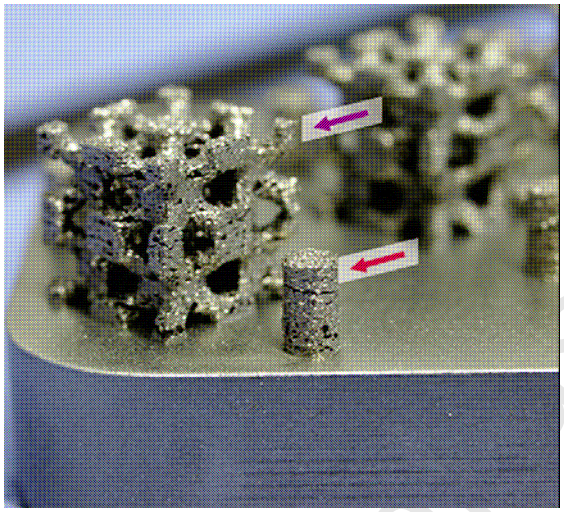

Figure 4.2. The structures formed via additive layer manufacturing by Pauly et al (2013) using powdered Fe –based bulk metallic glass on a 316 steel base plate.

There are multiple types of BMGs available today, all composed of different elemental contributions that result in variations in their glass forming abilities and thermal properties. The Al-based bulk metallic glass in particular has a low glass forming ability and a poor thermal stability. This has led to difficulties when attempting to increase the size of components produced. **Li et al (2014a)** exploited additive manufacturing using a laser for this material, introducing rapid heating and cooling cycles into small volumes of the material, thus overriding the issues surrounding its size limitations. The investigation was used to demonstrate the capability of laser melting to fabricate an Al-based bulk metallic glass and to determine the relationship between the laser parameters and the resulting microstructure and mechanical properties. Scanning was completed at four different lasers powers ranging from 80 W to 200 W. At higher values of power, the morphology of the track

created by the laser was influenced by the energy distribution of the beam. The value of the power also affects the strength of the resulting metallic glass; at higher powers, thermal stresses can be introduced into the system creating cracks, whereas lower powers will be insufficient to melt leading to a larger pore density. The authors concluded that there is a balance to be made when selecting laser power during laser melting. The power affects the thermal history of the scanned powder resulting in differing cooling rates depending on position of the energy distribution which results in varying morphologies over the scanned width. The research highlighted the difficulties introduced when using a system with many parametric options, the effects of which can highly influence the resulting mechanical properties.

4.3. Improving the quality of additive manufactured parts

These investigations demonstrated the feasibility of this technology to produce complex net-shaped components out of powder BMG using laser additive layer manufacturing. However, optimisation of parameters is still a current research issue in order to improve the quality of the final product.

Li et al (2014b) reported on the role of re-scanning using a lower energy density in order to improve the final net-shaped part. In particular, the aim was to halt the propagation of cracks formed during the building of the part as the thermal stresses from each layer accumulate. The authors tested this on cubes of Al-based BMG prepared using the same method as Pauly et al (2013) using a 1060 nm fibre laser operating at 200 W. After each layer preparation, the cubes were re-scanned using pulses with a lower power of 80 W. This method takes advantage of the property of BMGs whereby they exhibit superplasticity above the glass transition temperature. In this region, residual stress can be reduced by

viscous flow of the material without re-melting. The authors demonstrated the feasibility of this technique by producing micro gears out of Al-based bulk metallic glass that did not exhibit observable cracks associated with accumulation of these residual stresses. The part built with and without the rescanning technique can be seen in Figure 4.3. In particular, it can be observed from this figure that the propagation of the crack is halted when the layer is rescanned.

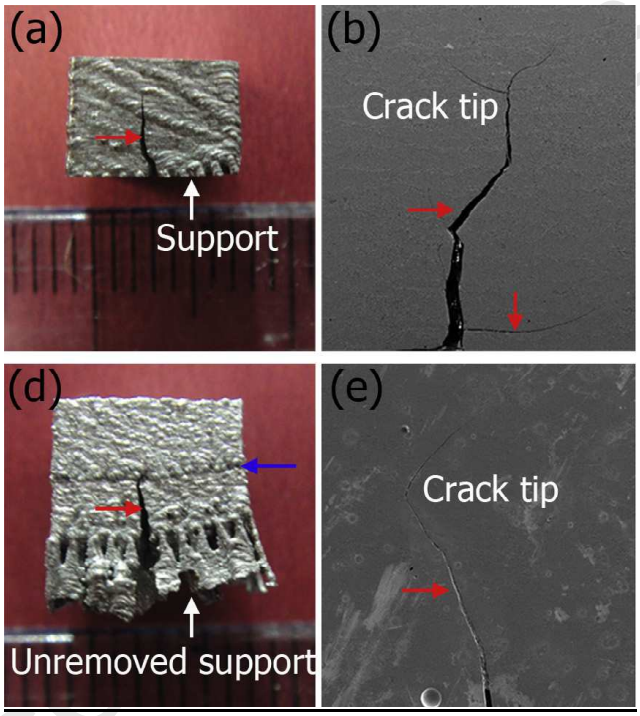

Figure 4.3. (a) and (d) are images of the parts created using ALM with (d) and without (a) a re-scan at a lower energy density. (b) and (e) are optical SEM inspections showing the halt in crack propagation when a layer is rescanned using a lower energy density before the next layer is deposited during ALM (Li et al 2014b).

Zhang et al (2015) used the pre-laid powder method over five layers processed with a 4 kW CO_2 laser operating at 10.6 µm to form a shape with the dimensions of 30 x 10 x 1.2 mm^3 over five layers. It was discovered that each layer presented a gradient structure consisting

of amorphous and nanocrystal microstructure. The authors concluded that these repeating microstructural patterns were due to the varying thermal histories experienced by each layer. Using temperature simulation, it was shown that the cooling rate decreases from the centre of the molten pool to the heat affected zone. At the centre of the molten pool, the cooling rate is high enough to supress crystallisation, but as the distance is increased the cooling rate becomes such that nanocrytsalline precipitates of the form $NiZr_2$ can grow (c.f Figure 4.4).

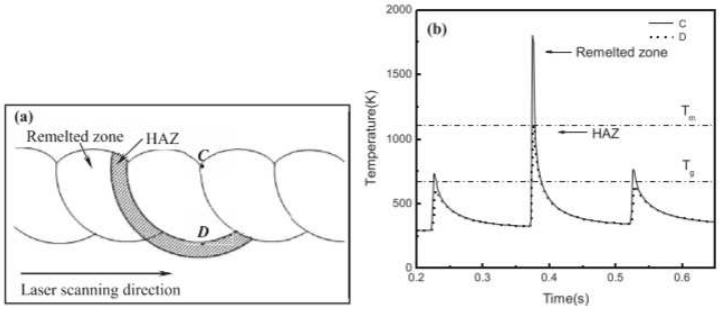

Figure 4.4. (a) Diagram of the deposition process in additive layer manufacturing and (b) the temperature profile as calculated theoretically for each section of the layer by Zhang et al (2015).

Also, within the heat affected zone, which does not experience melting, the temperature increase above the glass transition temperature is predicted to aid the formation of $Cu_{10}Zr_7$ dendrites, unlike the formation of the $NiZr_2$ phase which occurs due to solidification of the melt. The authors concluded that if each layer of molten bulk metallic glass powder can be cooled quickly enough before the deposition of the next layer, then amorphous BMG net shapes can be fabricated.

4.4. Simulation of additive manufacturing of bulk metallic glass

As with the other laser processing routes for BMG materials, simulation of ALM will also play an important role in understanding and controlling the cooling rates in the processes, and a review of publications on modelling to ALM is given in **Lavery et al 2014.** The main challenge in model development at this moment in time is in integrating the time and length scales, which require lasers operating at ms time-scales over tens of microns, to simulate melting and solidification of powders at the micro-level interacting with solid sublayers, and to cover much larger time (minutes) and length scales (tens of centimetres).

5. MICRO-MACHINING OF BULK METALLIC GLASS

5.1. Introduction to micro-machining

Although creating complex 3D parts out of BMGs is a current research topic, the results are not yet satisfactory. If components are created using other methods such as thermoplastic forming, they may still require post processing to induce surface textures or patterns. This can be achieved using lasers to machine on a micro- or nano-scale. The desirable mechanical properties of bulk metallic glass stem from their amorphous structure. This structure results in a lack of grain boundaries within the material sub-system. A lack of grain boundaries makes bulk metallic glass attractive for micromachining **(Kumar et al 2009).** It is therefore necessary to determine which parametric combinations result in retaining the initial amorphous structure of the BMG structure during laser micro-machining as well as producing a clean pattern at an acceptable removal rate.

5.2. Efficient micro-machining of bulk metallic glasses

With regards to an acceptable removal rate for the laser micro machining of bulk metallic glasses, **Sano et al (2007)** approached the question of whether there is a difference

between the removal of amorphous metallic glass compared to that of its' crystalline counterpart. Using a femtosecond laser operating at 800 nm and delivering pulses of 100 fs with between 2 and 900 μJ, the authors concluded that above an energy value of 10 μJ, material removal was lower for the crystallised sample than for that of the original bulk metallic glass. This difference was attributed to the presence of grain boundaries in the crystallised samples resulting in energy loss from electron during the femtosecond processing. **Wang et al (2007)** also concluded that the efficient micro machining of bulk metallic glasses can be conducted using femtosecond lasers. The authors identified that laser machining can be used to fabricate bulk metallic glass components with a high dimensional accuracy for application within the MEMS and sensor sectors of industry. Using a femtosecond laser also operating at 800 nm the authors determined the threshold of ablation for $Zr_{65}Cu_{17.5}Ni_{10}Al_{7.5}$ is 210 ± 9 $mJ.cm^{-2}$. The determination of the ablation threshold of the material was followed by the non-crystalline micro machining of holes and trenches with a variety of fluence values in the range of 5 – 25 $J.cm^{-2}$.This investigation displayed the potential for laser micro machining to be used as a technique for the non-crystalline machining of micro scale features in bulk metallic glasses.

Materials will respond differently to various parametric combinations and **Ma et al (2010)** and **Williams and Brousseau 2014** identified the need for systematic investigation of the response of bulk metallic glasses over a wider parametric range than studied by previous authors. **Williams and Brousseau (2014)** investigated the interaction of a 1064 nm nanosecond laser with Vitreloy 1 ($Zr_{41.2}Be_{22.5}Ti_{13.8}Cu_{12.5}Ni_{10}$) over a parametric range from 15 to 140 ns and for a variety of fluence values. The interaction was studied using single pulses. One of the main conclusions reached during this study, related to micro-machining, is that the cleanest craters are formed using shorter pulses (<25 ns). The authors used a thermal

model to deduce that at longer pulse lengths, the combination of the low thermal conductivity and melt temperature of these material results in more melt ejection surrounding the crater. This behaviour can be seen in Figure 5.1.

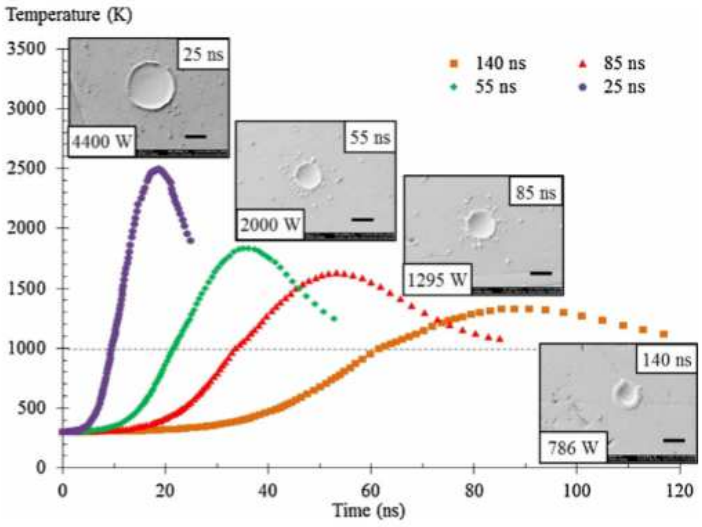

Figure 5.1. Theoretical evolution of temperature in a Zr-based bulk metallic glass irradiated by a 1064nm fibre laser at different pulse durations with accompanying SEM images of the pulses created (Williams and Brousseau, 2016).

Lin et al (2012) also studied nanosecond micro machining of bulk metallic glass. The authors used two different 30 ns lasers operating at 355 nm and 1064 nm to machine a Mg-based bulk metallic glass ($Mg_{65}Cu_{25}Gd_{10}$). Due to the material parameters, absorption of the 1064 nm laser was not sufficient to remove significant amounts of material making it unsuitable for the micro-machining of this particular metallic glass. The authors discovered specific parametric combinations that led to non-crystalline material removal (c.f figure 5.2). In particular, machining with a low power at a high scanning speed was found to be the parameters that resulted in retaining the amorphous structure.

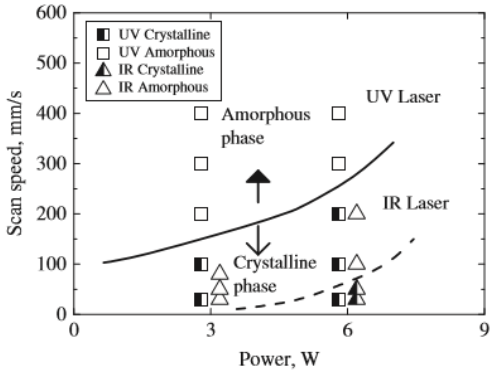

Figure 5.2. Machining parameters resulting in particular material response (Lin et al 2012).

5.3. Periodic structure formation during micro-machining of bulk metallic glass

Ma et al (2010) investigated the response of a different Zr-based bulk metallic glass ($Zr_{55}Al_{10}Ni_5Cu_{30}$) using a Ti-Sapphire femtosecond laser operating at 800 nm with a maximum pulse energy of 2 mJ. During this research, the authors observed concentric rings on the surface of the material machined. The authors identified three main types of ring structure coinciding with different parametric regimes. At a low laser power, the generated structure was attributed to non-thermal affects and as the power increased more evidence of thermal phenomena such as melting and material removal presented. Figure 5.3 identifies the parametric combinations necessary for the creation of the three various types of patterns observes during this work.

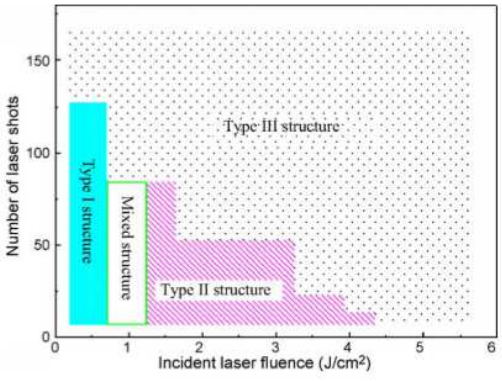

Figure 5.3. Graph identifying the incident laser fluence and the number of shots necessary to create specified structures as observed by Ma et al (2010).

Periodic structure created on the surface of bulk metallic glasses were also observed by other authors. **Liu et al (2011)** observed concentric surface ripples on the edges of Vitreloy 1 craters irradiated by a 10 ns pulse from a Nd:YAG laser operating at 532 nm. These patterns as shown in Figure 5.4 were attributed to the interference between the plasma created by irradiating at high laser intensity and the molten pool within the crater formed. **Liu et al (2012)** studied the interaction of the same material with the same laser but in a water environment. The authors observed the same phenomena but occurring around the crater edge with a star shaped pattern shown in Figure 5.5. The shape called 'Saffman-Taylor fingering' occurs due to the interaction of the plasma plume and the molten layer becoming unstable due to being in a liquid environment instead of air.

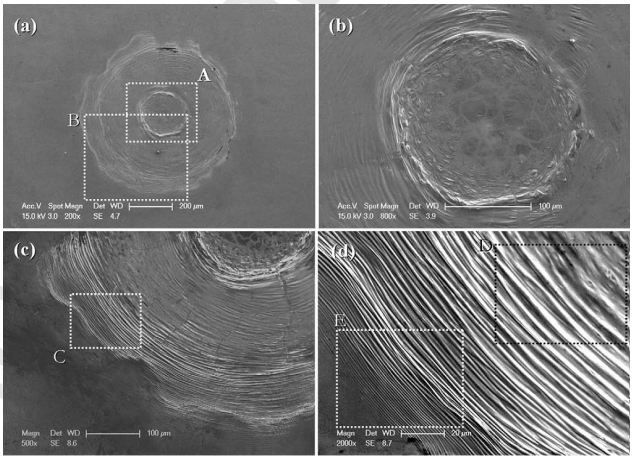

Figure 5.4. Morphology of Vitreloy 1 after being irradiated by a nanosecond laser operating at 532 nm and a pulse duration of 10 ns. The ripples are reported as being due to the interplay of two fluid layers with different density and horizontal velocity; the molten layer

induced by the laser heating and the subsequent plasma plume generated by ionisation of vaporised molecules (Liu et al, 2011).

Chen et al (2013) utilised these periodic structures for creating bulk metallic glass moulds for the imprint process. Using a Ti:sapphire laser operating at 800 nm and with a pulse duration of 180 fs, patterns were created in a Pd-based bulk metallic glass consisting of features of the order of magnitude from 100 µm to 90 nm. These moulds were then used as replication masters to imprint on polydimethylsiloxane (PDMS) and an Au-based bulk metallic glass. The authors concluded that the use of bulk metallic glass as a material for master moulds is advantageous due to the ease of the replication of micro features stemming from the homogenous structure of the material. Another advantage to using bulk metallic glasses is that the inherent high strength of these materials makes them suitable for use as moulds in the MEMS industry.

Zhu et al (2016) also studied the appearance of ripples on the surface of a Zr-based BMG using a 1064 nm Nd:YAG laser operating at 8ns in air. It was also concluded that these ripples occurred due to the Kevin-Helmholtz instability. By investigating the spatial geometry of the ripples with various energies it was determined that the spacing between the ripples is affected by the incident energy of the laser beam and also by how many pulses that are used to form the crater.

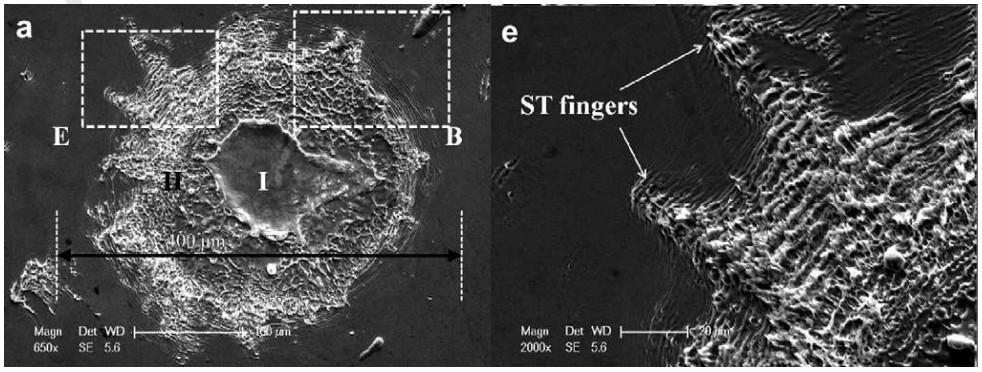

Figure 5.5. SEM micrographs of the surface morphology formed when the bulk metallic glass, Vitreloy 1, is ablated using a nanosecond laser, operating at 532 nm, with a single shot under water. The morphology is named 'Saffman-Taylor fingering' and is reported to occur due to the occurrence of an interface between the molten Vitreloy 1 layer and the expanding plasma plume which becomes unstable and causes the perturbation of waves within the original molten pool (Liu et al 2012).

6. IMPROVING THE MECHANICAL PROPERTIES OF BULK METALLIC GLASS THROUGH LASER PROCESSING

During laser processing of bulk metallic glasses, the material experiences an increase in free volume when its temperature is raised above the glass transition temperature and the residual stresses can be redistributed. Both of these factors can be exploited to improve the inherent brittleness of BMGs, which is one of the main restrictions when it comes to their widespread applications.

Chen et al (2010) observed an increase in the plasticity of a Zr-based bulk metallic glass after irradiation with a 180 W Nd:YAG laser. The sample that was treated using the laser did not fracture catastrophically, unlike its as-cast counterpart. Instead it deformed plastically after yielding, this behaviour can be seen in Figure 6.1. This behaviour was attributed to the re-distribution of residual stress during the laser heating process. This was further investigated by the same authors, **Chen et al (2012),** again using a Zr-based bulk metallic glass. These authors concluded that laser surface melting on the concave surface of a rectangular bar introduces tensile residual stress which balances the compressive stress introduced during

bending, increasing the overall strength of the bar. This conclusion was supported by the simulation of the residual stress on the material as seen in Figure 6.2.

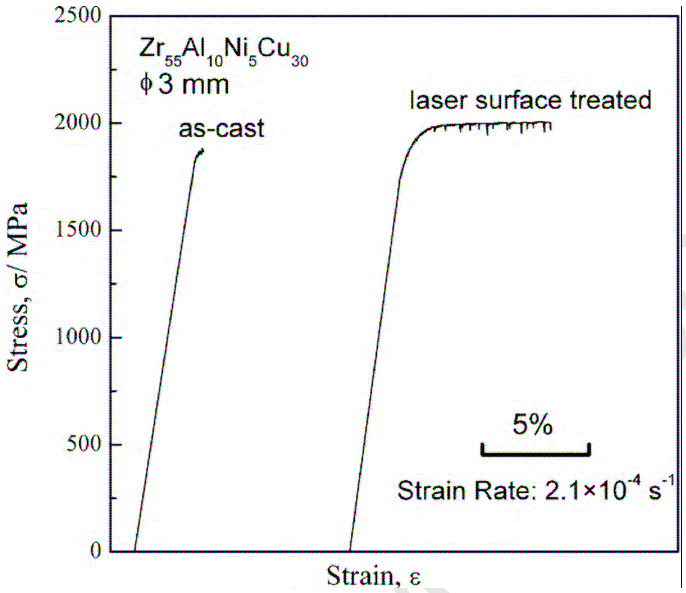

Figure 6.1. Stress-strain curve for untreated and laser treated Zr-based bulk metallic glass. The laser treated material does not fracture catastrophically unlike its' untreated counterpart (Chen et al, 2010.)

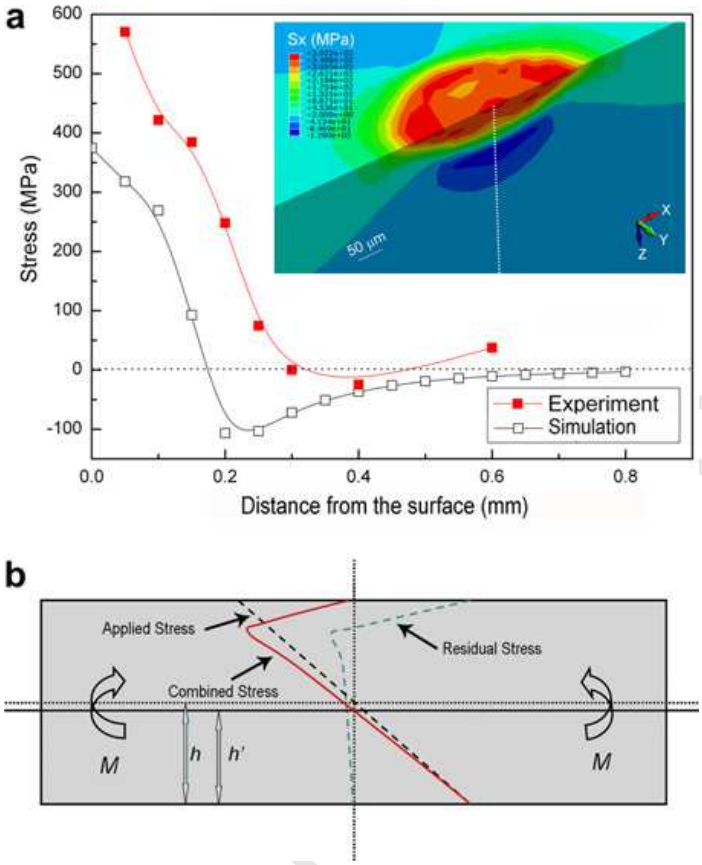

Figure 6.2 (a) Simulation of the residual stress on the surface of a laser treated BMG bar and (b) a schematic of the force during bending (Chen et al, 2012).

The residual stress induced during laser shock peening was reported by **Fu et al (2014),** using a nanosecond Nd:YAG laser to propagate a shock wave into a Zr-based BMG substrate. The shock wave-induced pressure may eventually exceed the yield strength of the material creating plastic deformation and resulting in favourable compressive residual stress being formed on the surface of the material. The authors analysed three samples; the as-cast BMG, a sample treated only on one side and a sample treated with laser shock peening on both sides. Of the three, the substrate treated on both sides displayed increased plasticity. The analysis agreed with the results of **Chen et al (2010)**; that laser shock peening induces a residual stress into the BMG and that this induced stress means that a higher load needs to be applied before the sample deforms.

Cao et al (2015) also reported on the laser shock peening of a Zr-based BMG, although with a different composition to that in the work of **Fu et al (2014).** The aim of these authors was to investigate the extent to which the laser shock peening of this material can affect its plasticity and its performance under compression testing, without the introduction of crystalline phases. By using water confinement, a plasma shock wave generated by irradiation of an aluminium coating on the surface of the BMG with a 1064 nm laser operating at 6 ns and 5 to 10 GW.cm^{-2} was introduced into the sample. It was concluded that the percentage of plastic elongation increased with intensity from 7 to 9 GW.cm^{-2} accompanied by an increase in fracture strengths as seen in Figure 6.3. The authors concluded that the laser shock peening of BMG can improve their ductility without affecting the surface topography.

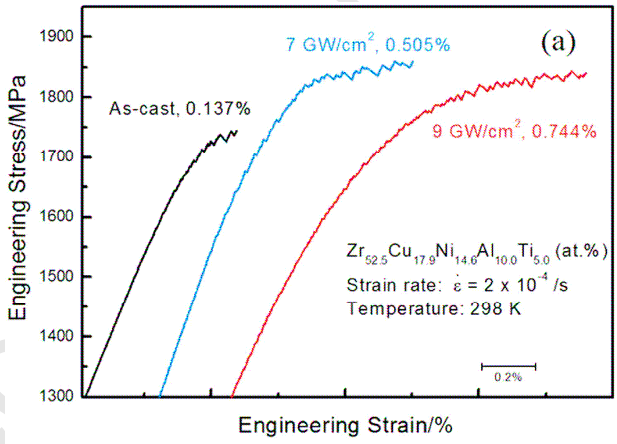

Figure 6.3. Stress strain curve of the samples treated with different laser intensities with fracturing occurring at the right hand side of the curve (Cao et al 2015).

The crystallisation that may occur during the laser machining of bulk metallic glass is not always viewed as a negative outcome. In particular, the controlled introduction of specific microstructures during laser machining can be an effective way to tailor the mechanical properties of the processed substrate. For example, **Wu et al (2012)** reported on the

hindrance of shear bands during stress-strain experiments when a Cu-based bulk metallic glass had been treated by a 180 W Nd:YAG laser. The reason behind this was the production of nano- and microcrystal precipitates forming a B2 CuZr phase throughout the depth of the processed area, which stopped the propagation of shear bands as can be seen in the SEM micrograph of Figure 6.4.

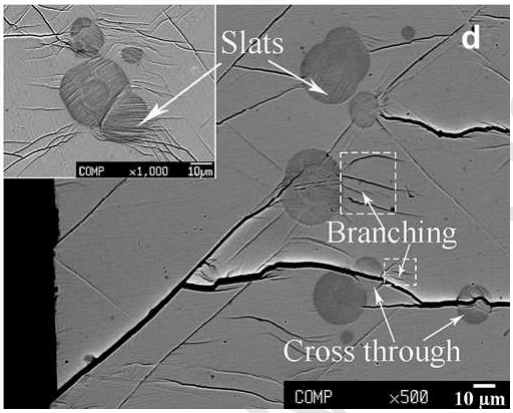

Figure 6.4. SEM micrograph displaying the propagation of shear bands being blocked by crystalline phases induced in Cu-based BMG after laser treatment (Wu et al 2012).

Fornell et al (2014) discovered that the surface laser texturing of a Cu-based ($Cu_{47.5}Zr_{47.5}Al_5$) bulk metallic glass at specific values of intensities has an effect on the hydrophobicity of the surface. The surfaces of the bulk metallic glass samples were irradiated with a low power Nd:YVO_4 laser operating in the infrared regime and in the continuous mode. The results from the samples processed with different intensities (28.5A, 29A and 30A) showed that at higher intensities, the increased surface roughness as well as the larger oxide content which increased the chances of a water molecule bonding with the oxygen resulted in better wettability of the surface. This conclusion was supported by images of an NaCl droplet on the surfaces of each irradiated BMG part as seen in Figure 6.5.

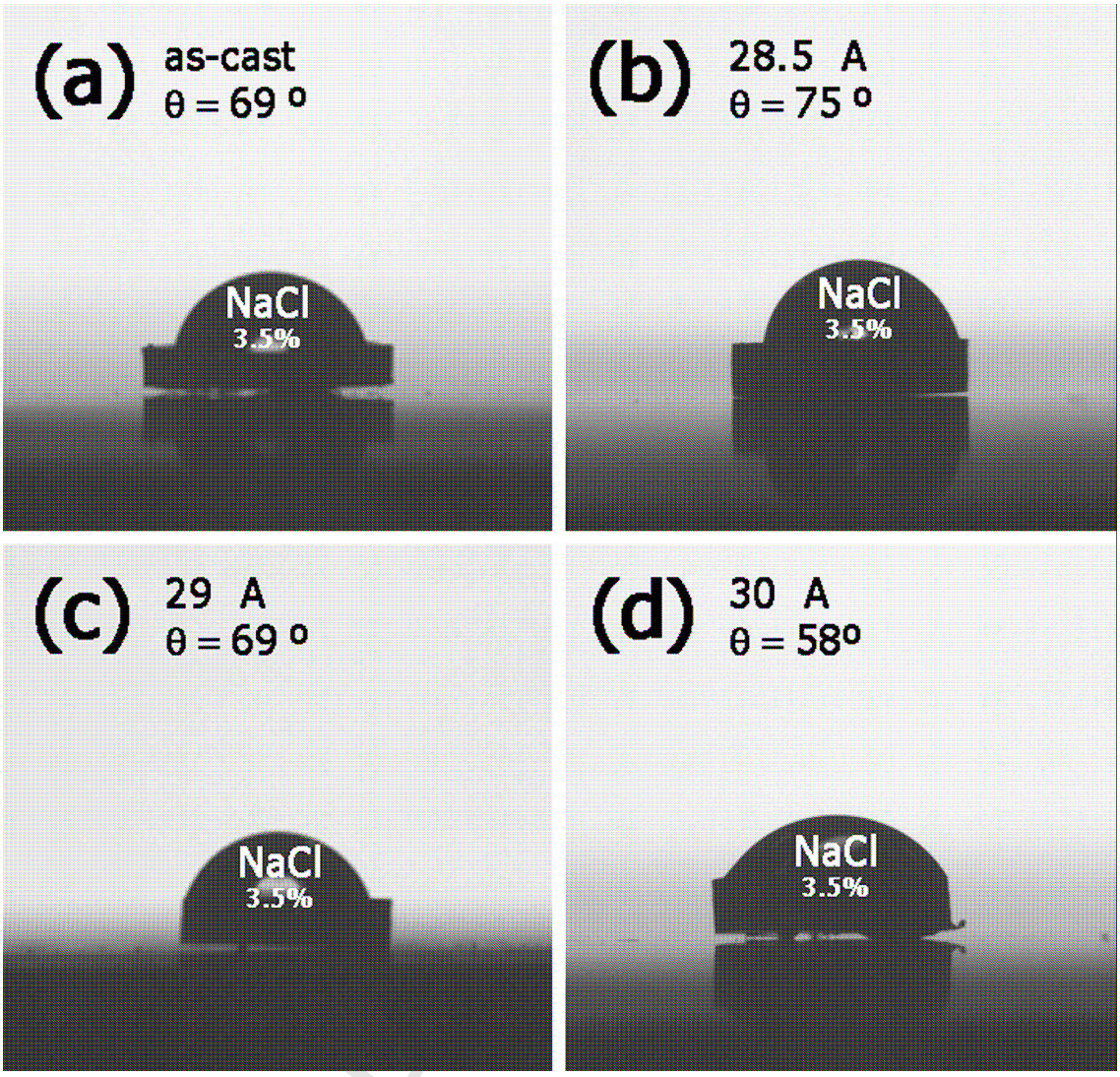

Figure 6.5. NaCl droplets on the surfaces of Cu-based BMG surfaces each treated with different laser intensities (Fornell et al, 2014).

The authors also concluded, in agreement with **Wu et al (2012)**, that the crystallinity of the laser treated sample aided in the restriction of shear band propagations when the sample is subjected to a load, thus improving the plasticity of the material. On the subject of plasticity improvement, **Gao et al (2016)** introduced the concept that laser surface texturing treatment could be used as a way to improve the plasticity of a Zr-based bulk metallic glass. Using picosecond lasers to texture the surface of the material with varying sized arrays of

pores, the authors showed that the pores are comparable to soft crystalline phases in aiding in the stress distribution when the BMG is under strain. This results in the prevention of the propagation of major shear bands within the material.

7. CONCLUSIONS AND FUTURE OUTLOOK

This review reported the wide range of laser processing applications of bulk metallic glasses, indicating the potential capabilities for a number of industrially relevant processes. It showed the capability of lasers to be able to keep up with the demands of advanced materials engineering. In particular, the high heating and cooling rates inherent to laser applications make them attractive to process metallic glasses due to the critical thermal constraints associated with the retainment of their amorphous structure. Although research efforts surrounding the laser processing of bulk metallic glass have increased in the past decade, this field of studies is still in its infancy. The following conclusions are made for each of the reviewed laser processing applications:

LASER WELDING It would appear that laser welding can be successful in joining metallic glasses together without compromising their amorphous structure resulting in a strong bonding technique that can side-step the size restrictions imposed by the synthesis of bulk metallic glasses. Previous research has identified relationships between parametric variation and the resulting microstructure of a number of bulk metallic glasses. Although successful welding has been demonstrated, it is only recently that researchers have begun to use thermal modelling and simulation in an attempt to predict crystallisation during laser welding. Such theoretical work is necessary however due to the wide range of available laser systems which exhibit different operating windows as well as the vast amount of different bulk metallic glasses, a number that is set to increase within the coming years.

LASER CLADDING/COATING Laser cladding using bulk metallic glass powders shows promise to enhance the surface properties of a range of materials. This technique has been shown to increase the hardness and corrosion resistance of tribologically poor materials. However, the research results presented in current studies indicates that it is difficult to achieve truly amorphous coatings. This can affect the lifetime performance of the coating. Thus, this is an avenue for refinement through further investigations. The literature reviewed also highlights the numerous parameters that need to be considered when cladding bulk metallic glasses such as scanning speed and laser power as well as the scanning speed during the second step of laser re-melting.

ADDITIVE LAYER MANUFACTURING The additive layer manufacturing of bulk metallic glasses is still a relatively young research field. Even though such studies are comparatively scarce, the layer-by layer melting process of metallic glass powder has shown great promise to form sophisticated geometries without the cooling times restrictions or limiting the process time when accessing the super cooled liquid region during thermoplastic forming. Using lasers to melt layer by layer results in a cooling cycle limited to each layer allowing more flexibility to bypass the crystallisation regime. Furthering the simulation capabilities within this field to include multiple length scales may aid in the control of cooling rates across complex 3D geometries. There are still issues within this research area, such as the tendency of BMG structures to fail due to residual stress during processing. However, techniques such as using a second lower energy laser scan are being developed to address this. There is also the possibility of designing support structures for the manufactured part that can aid in its cooling further securing the integrity of the 3D design.

MICROMACHINING The lack of large scale grain boundaries in bulk metallic glasses makes them an ideal candidate for machining on a nano and micro scale. Investigations of the interaction of bulk metallic glasses with laser operating in the femto and nano second regimes have produced fundamental information on the micromachining thresholds as well as the onset of crystallisation. Patterns that can be utilised for nanoimprint masters have been found to result at specific energies using a laser operating in the femtosecond regime. Research on the reaction of bulk metallic glasses to laser irradiation at a micro scale can be utilised for applications such as machining medical devices including stents and surgical instruments, and as the interest in creating biocompatible bulk metallic glasses increases, there becomes a necessity for a tool that is capable of processing them. With further development of bulk metallic glass compositions it will be necessary to continue to investigate the use of lasers to irradiate at a micro scale to be able to apply them to industrial applications. Also, it is important to continue to identify laser system parameters that result in efficient micro machining of a variety of bulk metallic glasses. In particular those parameters that result in carefully controlled removal of material without damaging the surrounding areas of the material.

PROPERTY VARIATION Finally, lasers provide a method for tuning the properties of bulk metallic glasses in a selective manner. Researchers have demonstrated the ability to improve the plasticity of the material by introducing favourable residual stresses through laser shock peening. This method has been shown to maintain the amorphous structure of the processed part. In addition, induced nano-crystallisation has also demonstrated the desirable effect of hindering shear bands formed under loading. Laser texturing of the bulk metallic glass surface has also been proven to increase its hydrophobicity.

Based on the reviewed studies, it can be said that the laser processing of bulk metallic glass is a powerful tool capable of many processing routes and outcomes. However, there are still many challenges that deserve further research:

- The nature of laser material interaction varies depending on the type of material as well as the kind of laser system utilised. As the development of lasers continues and the amount of available bulk metallic glasses increases, the demand for sound, comprehensive research will continue. Understanding the fundamental interaction of laser energy with multi-component alloys will be necessary as well as proof of concept for the different laser processing applications in order to promote the wider utilisation these materials.

- In addition, the crystallisation kinetics of bulk metallic glasses during laser irradiation needs to be understood to aid in the development and optimisation of processes such as welding and cladding. The onset of crystallisation could be predicted using the intersection of the continuous heating curve and the temperature field simulations. An accurate simulation is not a minor challenge, developing a complete temperature field model during laser irradiation is a complex task when considering vaporisation, plasma effects as well as chemical composition changes in the material. Besides, there is also the issue of variations in material properties as the temperature increases, particularly for BMGs whose temperature dependent properties are not well-documented.

- The research into the additive layer manufacturing of bulk metallic glass should continue to grow. The research has shown the potential of this technique to

manufacture components with the attractive properties of bulk metallic glass, whilst removing the barriers imposed by other processing techniques. This results in the possibility of a processing route with the capability of forming complicated geometrical amorphous structures. Parametric effects need to be addressed to complete the optimisation of this process. For example, the influence of the energy distribution on the melt flow has not been thoroughly researched. Further investigations of the resulting crystallisation processes upon repeated melting and solidification should also aid in the process being able to be controlled more effectively.

- Finally, the use of laser processing of bulk metallic glass for specific application needs to be investigated further such as structural applications of laser welded BMG parts or the use of micro-machined bulk metallic glass components in industrial applications. Such technology demonstrators can help in the wider adoption of BMGs in different industrial sectors.

Acknowledgements.

The Authors gratefully acknowledge the financial support provided by the Welsh Government and Higher Education Funding Council for Wales through the Sêr Cymru National Research Network in Advanced Engineering and Materials

References.

Anantharaman, T.R. 1984. *Metallic Glasses – Production, Properties and Applications.* Trans Tech Publications Ltd.

Axinte, E. 2012. Metallic Glasses from “Alchemy” to Pure Science: Present and Future of Design, Processing and Applications of Glassy Metals. *Materials and Design* 35, pp. 518 - 556

Cao, Y., Xie, X., Antonaglia, J., Winiarski, B., Wang, G., Shin, Y.C., Withers, P.J., Dahmen, K.A. and Liaw, P.K. 2015. Laser Shock Peening of Zr-based Bulk Metallic Glass and Its Effect on Plasticity: Experiment and Modeling. *Nature: Scientific Reports 5 Article number 10789*

Chen, B., Li, Y., Yi, M., Li, R., Pamg, S., Wang, H. and Zhang, T. 2012. Optimization of mechanical properties of bulk metallic glasses by residual stress adjustment using laser surface melting. *Scripta Materialia,* 66(12) pp. 1057-1060.

Chen, B., Pang, S., Han, P., Li, Y., Yavaru, A.R., Vaughan, G. and Zhang, T. 2010. Improvement in mechanical properties of a Zr-based bulk metallic glass by laser surface treatment. *Journal of Alloys and Compounds,* 504(1) pp. 545-547.

Chen, B., Shi, T., Li, M., Wen, C. and Liao, G. 2015. Crystallization of $Zr_{55}Cu_{30}Ni_5Al_{10}$ Bulk Metallic Glass in Laser Welding: Simulation and Experiment. *Advanced Engineering Materials,* 17(4) pp. 483-490.

Chen, B., Shi, T.L., Li, M., Yang, F., Yan, F. and Liao, G.L. 2014. Laser welding of annealed $Zr_{55}Cu_{30}Ni_5Al_{10}$ bulk metallic glass. *Intermetallics,* 46 pp. 111-117.

Chen, Y.C., Chu, J.P., Jang, J.S.C., Hsieh, C.W., Yang, Y., Li, C.L., Chen, Y.M. and Jeng, J.Y. 2013. Replication of nano/micro-scale features using bulk metallic glass mold prepared by femtosecond laser and imprint process. *Journal of Micromechanics and Microengineering,* 23(3).

Dawes, C. 1992. *Laser Welding: A Practical Guide,* Woodhead Publishing.

Fornell, J., Pellicer, E., Garcia-Lecina, E., Nietro, D., Surinach, S., Baro, M.D. and Sort, J. 2014. Structural and mechanical modifications induced on $Cu_{47.5}Zr_{47.5}Al_5$ metallic glass by surface laser treatments. *Applied Surface Science,* 290 pp. 188-193/

Fu, J., Zhu, Z., Zheng, C., Liu, R. and Ji, Z. 2014. Effect of laser shock peening on mechanical properties of Zr-based bulk metallic glass. *Applied Surface Science,* 313 pp. 692-697.

Gao, M., Dong, J., Huan, Y., Wang, Y, T. And Wang, W-H. 2016. Macroscopic tensile plasticity by scalarizating stress distribution in bulk metallic glass. *Scientific Reports,* 6 Article Number 21929.

Greer, A, L. 2015. New horizons for glass formation and stability. *Nature Materials,* 14, pp. 542 – 546.

Inoue A., Wang X.M. and Zhang W. 2008. Developments and Applications of Bulk Metallic Glasses. *Reviews on Advanced Materials Science*, 18(1) pp. 1-9.

Inoue, A. and Takeuchi, A. 2011. Recent developments and application products of bulk glassy alloys. *Acta Materialia,* 59 pp. 2243–2267.

Kawahito, Y., Terajima, T., Kimura, H., Kuroda, T., Nakata, K., Katayama, S. and Inoue, A. 2008. High-power fiber laser welding and its application to metallic glass $Zr_{55}Al_{10}Ni_5Cu_{30}$. *Materials Science and Engineering B,* 148(1-3) pp. 105-109.

Khan, M.M.A., Romoli, L., Fiaschi, M., Dini, G. and Sarri, F. 2011. Experimental design approach to the process parameter optimization for laser welding of martensitic stainless steels in a constrained overlap configuration. *Optics and Laser Technology,* 43(1) pp. 158-172.

Kim, J., Lee, D., Shin, S. and Lee, C. 2006. Phase evolution in $Cu_{54}Ni_6Zr_{22}Ti_{18}$ bulk metallic glass Nd:YAG laser weld. *Materials Science and Engineering A* 434, pp. 194-201

Klement W., Willens R.H. and Duwez P. 1960. Non-Crystalline Structure in Solidified Gold–Silicon Alloys. *Nature*, 187 pp. 869-870.

Kumar G., Tang H.X. and Schroers J. 2009. Nanomoulding with Amorphous Metals. *Nature*, 457 pp. 868-872.

Lavery, N.P., Brown, S.G.R., Sienz, J. and Belblidia, F. 2014. A Review of Computaional Modelling of Additive Layer Manufacturing – Multi-Scale and Multi-Physics. *International Conference of Sustainable Design and Manufacturing*, Cardiff, Wales 28-30 April 2014.

Li B., Li Z.Y., Xiong J.G., Xing L., Wang D. and Li Y. 2006. Laser Welding of $Zr_{45}Cu_{48}Al_7$ Bulk Glassy Alloy. *Journal of Alloys and Compounds*, 413(1-2) pp. 118-121.

Li, R., Jin, Y., Li, Z., Zhu, Y. and Wu, M. 2014. Effect of remelting scanning speed on the amorphous forming ability of Ni-based alloy using laser cladding plus a laser remelting process. *Surface and Coatings Technology,* 259(C) pp.725-731.

Li, R., Li, Z., Huang, J., Zhang, P. and Zhu,Y. 2011. Effect of Ni-to-Fe ration on structure and properties of Ni-Fe-B-Si-Nb coatings fabricated by laser processing. *Applied Surface Science,* 257 pp. 3554-3557.

Li, R., Li, Z., Zhu, Y. and Qi.K. 2013. Structure and corrosion resistance properties of Ni-Fe-B-Si-Nb amorphous composite coatings fabricated by laser processing. *Journal of Alloys and Compounds,* 580 pp. 327-331.

Li, X.P., Kang, C.W., Huang, H. and Sercombe, T.B. 2014b. The role of a low-energy-density re-scan in fabricating crack-free $Al_{85}Ni_5Y_6Co_2Fe_2$ bulk metallic glass composites via selective laser melting. *Materials and Design,* 63 pp. 407-411.

Li, X.P., Kang, C.W., Huang, H., Zhang, L.C. and Sercombe, T.B. 2014a. Selective laser melting of an $Al_{86}Ni_6Y_{4.5}Co_2La_{1.5}$ metallic glass: Processing, microstructure evolution and mechanical properties. *Materials Science and Engineering A,* 606 pp. 370-379.

Lin, H-K., Lee, C-J., Hu, T-T., Li, C-H. and Huang, J.C. 2012. Pulsed laser micromachining of Mg-Cu-Gd bulk metallic glass. *Optics and Lasers in Engineering,* 50(6) pp. 883-886.

Liu Y., Jiang M.Q., Yang G.W., Guan Y.J. and Dai L.H. 2011. Surface Rippling on Bulk Metallic Glass under Nanosecond Pulse Laser Ablation. *Applied Physics Letters* 99(19) 191902.

Liu, Y., Jiang, M.Q., Yang, G.W., Chen, J.H., Guan, Y.J and Dai, L.H. 2012. Saffman-Taylor fingering in nanosecond pulse laser ablating bulk metallic glass in water. *Intermetallics,* 31 pp. 325-329.

Lu, Z.P. and Liu, C.T. 2004. Role of minor alloying additions in formation of bulk metallic glasses: A Review. *Journal of Materials Science,* 39(12) pp. 3965-3974.

Ma, F., Yang, J., Zhu, X., Liang, C. and Wang, H. 2010. Femtosecond laser-induced concentric ring microstructures on Zr-based metallic glass. *Applied Surface Science,* 256(11) pp. 3653-3660.

Matthews, D.T.A., Ocelik, V. and de Hosson, J.Th.M. 2007. Tribological and mechanical properties of high power laser surface-treated metallic glasses. *Materials Science and Engineering A* 471, pp. 155-164.

Otsu, M., Ide, Y., Sakurai, J., Hata, S. And Takashima, K. 2009. Laser Forming of Thin Metallic Glass. *Journal of Solid Mechanics and Materials Engineering,* 3(2) pp. 387-396.

Pauly, S., Lober, L., Petters, R., Stoica, M., Scudino, S., Kuhn, U. and Eckert, J. 2013. Processing metallic glasses by selective laser melting. *Materials Today,* 16(1/2) pp. 37-41.

Peker, A. and .Johnson, W.L. 1993. A highly processable metallic glass: $Zr_{41.2}Ti_{13.8}Cu_{12.5}Ni_{10.0}Be_{22.5}$. *Applied Physics Letters* 63 (17), pp. 2342-2344

Sano, T., Takahashi, K., Hirose, A. and Kobayashi, K.F. 2007. Femtosecond Laser ablation of $Zr_{55}Al_{10}Ni_5Cu_{30}$ Bulk Metallic Glass. *Materials Science Forum,* 539-543 pp. 1951-1954.

Schroers J., Pham Q. and Desai A. 2007. Thermoplastic Forming of Bulk Metallic Glass - A Technology for MEMS and Microstructure Fabrication. *Journal of Microelectromechanical Systems* 16 (2), pp 240-247.

Schroers, J. 2010. Processing of Bulk Metallic Glass. *Advanced Materials,* 22(14) pp. 1566-1597.

Schroers, J., Kumar, G., Hodges, T.M., Chan, S. and Kyriakides, R. 2009. Bulk metallic glasses for biomedical applications. *JOM* 61 (9), pp. 21 – 29

Toyserkani, E., Khajepur, A. and Corbin, S.F. 2004. *Laser Cladding*, CRC Press.

Wang, G., Huang, Y.J., Shagiev, M. and Shen, J. 2012. Laser welding of $Ti_{40}Zr_{25}Cu_{12}Be_{20}$ bulk metallic glass. *Materials Science and Engineering A,* 542 pp. 33-37.

Wang, H-S., Chen, H-G. and Jang, J.S-C. 2010. Microstructure evolution in Nd:YAG laser-welded $(Zr_{53}Cu_{30}Ni_9Al_8)Si_{0.5}$ bulk metallic glass alloy. *Journal of Alloys and Compounds*, 495 pp. 224-228.

Wang, H.S., Chen, H.G., Jang, J.S.C. and Chiou, M.S. 2010b. Combination of a Nd:YAG laser and a liquid cooling device to $(Zr_{53}Cu_{30}Ni_9Al_8)Si_{0.5}$ bulk metallic glass welding. *Materials Science and Engineering A,* 528 pp. 338-341.

Wang H.S., Choiu, M.S., Chen, H.G. and Jang, J.S.C. 2011. The effects of initial welding temperature and welding parameters on the crystallization behaviours of laser spot welded Zr-based bulk metallic glasses. *Material Chemistry and Physics,* 129 pp. 547-552.

Wang, H-S., Su, Y-Z., Jang, J.S-C. and Chen, H-G. 2013. A comparison of crystallization behaviours of laser spot welded Zr-Cu-Ag-Al and Zr-Cu-Ni-Al bulk metallic glasses. *Materials Chemistry and Physics,* 139(1) pp. 215-219.

Wang, Y., Li, G., Wang, C., Xia, Y., Sandip, B. and Dong, C. 2004. Microstructure and properties of laser clad Zr-based alloy coating on Ti substrates. *Surface and Coatings Technology,* 176 pp. 284-289.

Wang, H.S., Wu, J.Y. and Liu, Y.T. 2016. Effect of volume fraction of the *ex-situ* reinforced Ta additions on the microstructure and properties of laser-welded Zr-based bulk metallic glass composites. *Intermetallics*, 68 pp. 87-94.

Williams, E and Brousseau, E.B. 2016. Nanosecond laser processing of $Zr_{41.2}Ti_{13.8}Cu_{12.5}Ni_{10}Be_{22.5}$ with single pulses. *Journal of Materials Processing Technology, 232* pp. 34-42.

Wong, T.T. and Liang, G.Y. 1997. Formation and Crystallization of Amorphous Structure in the Laser-Cladding Plasma-Sprayed Coating of Al-Si Alloy. *Materials Characterization,* 38 pp. 85-89.

Wong, T.T., Liang, G.Y., He, B.L. and Woo, C.H. 2000. Wear resistance of laser-clad Ni-Cr-B-Si alloy on aluminium alloy. *Journal of Materials Processing Technology,* 100 pp. 142-146.

Wu, G., Li, R., Liu, Z., Chen, B., Li, Y., Cai, Y. and Zhang, T. 2012. Induced multiple heterogeneities and related plastic improvement by laser surface treatment in CuZr-based bulk metallic glass. *Intermetallics*, 24 pp. 50-55.

Wu, X. and Hong, Y. 2001. Fe-based thick amorphous-alloy coating by laser cladding. *Surface and Coatings Technology,* 141 pp. 141-144.

Xia, C., Xing, L., Long, W-Y., Li, Z-Y. and Li, Y. 2009. Calculation of crystallization start line for $Zr_{48}Cu_{45}Al_7$ bulk metallic glass at a high heating and cooling rate. *Journal of Alloys and Compounds,* 484 pp. 698-701.

Yang, G., Lin, X., Liu, F., Hu, Q., Ma, L., Li, J. and Huang, W. 2012. Laser solid forming Zr-based bulk metallic glass. *Intermetallics,* 22 pp.110-115.

Yue, T.M., Su, Y.P. and Yang, H.O. 2007. Laser cladding of $Zr_{65}Al_{7.5}Ni_{10}Cu_{17.6}$ amorphous alloy and magnesium. *Materials Letters,* 61 pp. 209-212.

Zhang, Y., Lin, X., Wang, L., Wei, L., Liu, F. and Huang, W. 2015. Microstructural analysis of $Zr_{55}Cu_{30}Al_{10}Ni_5$ bulk metallic glasses by laser surface remelting and laser solid forming. *Intermetallics,* 66 pp. 22-30.

Zheng, C., Sun, S., Song, L., Zhang, G., Luan, Y., Ji, Z. And Zhang, J. 2013. Dynamic fracture characteristics of $Fe_{78}Si_9B_{13}$ metallic glass subjected to laser shock loading. *Applied Surface Science,* 286 pp. 121-125.

Zhu, Y.Y., Li, Z.G., Li, R.F., Li, M., Daze, X.L., Feng, K. and Wu, Y.X. 2013. Microstructure and property of Fe-Co-B-Si-C-Nb amorphous composite coating fabricated by laser cladding process. *Applied Surface Science,* 280 pp.50-54.

Zhu, Y., Fu, J., Zheng, C. and Ji, Z. 2016. Effect of nanosecond pulse laser ablation on the surface morphology of Zr-based metallic glasses. *Optics and Laser Technology,* 83 pp. 21-27.

Appendix

er	Material	Laser Pulse Duration	Laser Power or Energy	Scanning Speed	Crystal?	Precipitates
lding						
t al 06)	$Zr_{45}Cu_{48}Al_7$	N/A	1200W	2 to 8 m.min-1	Yes	τ_5 , ZrCu and unknown precipitates.
n et al 06)	$Cu_{54}Ni_6Zr_{22}Ti_{18}$	1-10 ms	0.5 - 4 kW	20 - 60 mm/min	Yes	Crystalline precipitates not identified but % of copper content increases with welding
vahito et 2008)	$Zr_{55}Al_{10}Ni_5Cu_{30}$	Continuous Wave	2-10 kW	48 and 72 $m.min^{-1}$	N/A	N/A
ng et al 10).	$Zr_{53}Cu_{30}Ni_9Al_8Si_{0.5}$	4.5- 5.9 ms	5.5 - 7 J	60 mm/min	Yes	Precipitates rich in Zr, Ni and Cu with particle sizes from 30 to 200 nm.
ng et al 12)	$Ti_{40}Zr_{25}Ni_3Cu_{12}Be_{20}$		3.5 kW	6 to 10 $m.min^{-1}$		
ng et al 13)	$Zr_{53}Cu_{30}Ni_9Al_8Si_{0.5}$/ $Zr_{48}Cu_{36}Ag_8Al_8Si_{0.75}$	4.5 ms	1.8 - 2.4 kW	N/A	Yes	Zr_2Cu
ng et al 16)	$Zr_{48}Cu_{36}Ag_8Al_8Si_{0.5}$	4.5 ms	1.9 kW	60 mm/min	Yes	Zr_2Cu and $Zr_{10}Cu_7$
ng et al 10_b)	$Zr_{53}Cu_{30}Ni_9Al_8Si_{0.5}$	6 ms	7 J	60 mm/min	Yes	Zr_2Cu
ang et al 1)	$Zr_{53}Cu_{30}Ni_9Al_8Si_{0.6}$	4.5 ms	5 - 8 J	N/A	Yes	Zr_2Cu major phase in HAZ
en et al 14)	$Zr_{55}Cu_{30}Ni_5Al_{10}$	Continuous	1.5 - 2.1 kW	8 - 10 m/min	Yes	Not identified
dding						
and ng (2001)	Fe-based	N/A	7.5 kW	50 mm/s	No	
ng et al	Zr-based		1.4 kW	$4mm.s^{-1}$	Yes	Mainly of

04)						Zr- bonded phases such as Zr3Al2
e et al 07)	$Zr_{65}Al_{7.5}Ni_{10}Cu_{17.5}$	Continuous Wave	3.2 kW	5 mm/s	No	Amorphous up tp 1.1 mm
t al 11)	Ni-Fe-Si-B-Nb (four diffferent powders with 45, 50, 55 and 60% Nb)	N/A	1st - 5.5 kW, 2nd - 14 kW	1st - 400 mm/min, 2nd - 8000 mm/min	Yes	NbC particulates and γ(Fe,Ni)
u et al 13)	Fe-based	N/A	1200 W	17mm.s^{-1}	Yes but amorphous content of 87.6%	Majority of crystalline particles were of the form NbC
t al 13)	$Ni_{40.8}Fe_{27.2}B_{18}Si_{10}Nb_4$	N/A	0.8 kW	360 mm/min	Yes	NbC particulates and γ(Fe,Ni)
t al 14)	Ni-based	N/A	0.8 kw and 3.5 kW	4m.min^{-1} and 8 m.min^{-1}	Yes	NbC particulates and γ(Fe,Ni)
M						
g et al 12)	Zr-based	3 ms	80 J		Amorphous contents being relatively high, at 92.44%	$Al_5Ni_3Zr_2$
ly et al 13)	Fe-based	N/A	320 W	3470 mm.s^{-1}	Not entirely amorphous, it was no different than the original powder feedstock used in its creation	
t al 14a)	Al-based	N/A	80 W to 200 W	N/A	Yes	Al crystals identified

						and others not identified
t al 14b)	Al-based	N/a	200 W (re-scan at 80 W)	625 mm/s	Not entirely amorphous, it was no different than the original powder feedstock used in its creation	
ng et al 15					Nanocrytsalline precipitates of the form NiZr3 AND formation of Cu10Zr7 dendrites within the heat affected zone	
cro-chining						
o et al 07)	$Zr_{55}Al_{10}Ni_5Cu_{30}$	100 fs	between 2 and 900 µJ	N/A	Not studied	
ng et al 07)	$Zr_{65}Cu_{17.5}Ni_{10}Al_{7.5}$	50 fs	2 mJ	N/A	Not studied	
liams l usseau 16	$Zr_{41.2}Be_{22.5}Ti_{13.8}Cu_{12.5}Ni_{10}$	15 - 140 ns	4.9 J/cm - 43.7 J/cm	N/A	Not Studied	
et al 12)	$Mg_{65}Cu_{25}Gd_{10}$	30 ns	1 to 9 W	Up to 350 mm/s	Non-crystalline material removal	
et al 10)	$Zr_{55}Al_{10}Ni_5Cu_{30}$	50 fs	0.18 J/cm - 5.3 J/cm	Single pulses	Not studied	
et al 11)	$Zr_{41.2}Be_{22.5}Ti_{13.8}Cu_{12.5}Ni_{10}$	10 ns	238 J/cm	Single pulses	Not studied	
n et al 13)	Pd-based	180 fs	100 mW	Single pulses	Not studied	

u et al 16)	Zr-based	8 ns	200 - 600 mJ	Single pulses	Not studied	
proving perties						
en et al 10)	Zr-based		180 W	1000 mm/min	None	
et al 14)	Zr-based	11 ns	400 mJ		None	
o et al 15)	Zr-based	6 ns	5 to 10 $GW.cm^{-2}$			
et al 12)	Cu-based	1 ms	180 W	200 mm/min	Yes	Nano- and microcrystal precipitates forming a B2 CuZr phase
nell et al 14)	$Cu_{47.5}Zr_{47.5}Al_5$	Continuous Wave	28.5A 29A 30a	10 mm/s	Yes	B2 CuZr and ZrO2